

Supplementary Materials: Developmental Control of *NRAMP1* (*SLC11A1*) Expression in Professional Phagocytes

Mathieu F. M. Cellier

Correlating CAGE signals and other marks of *NRAMP1* expression in AMLs.

The area spanning *NRAMP1* exons XIII-XV that comprises DHS F10 and F3 [11] is heavily decorated with K9/27ac and K4me2/3 in K562 cells, whereas CD14⁺MNs show strong marking with K4me1 only (Figure S2B). Histone modifications thus appear consistent with CAGE data (Figure S1B), suggesting that RNA Pol II activity at the 3' end of *NRAMP1* Orf may coincide with absence of full-length gene expression in myeloid cell types either divergent from the myelo-monocytic fate (such as K562 cells) or representing some transformed, aberrant progenitor stage (e.g., NB4 APL, Figure 1). In contrast, RNA Pol II activity at *NRAMP1* TSS characterizes cells either expressing or prone to express *NRAMP1*, such as CD14⁺MNs and HL-60 cells, respectively.

Along these lines, the area of *NRAMP1* exon XV comprises DNase footprint F3 found in both megakaryocytic progenitors and CMPs that matches a potential binding site for ELF1 revealed by ChIP-seq (see text section 2.3.1.7.). Given ELF1 involvement in gene regulation in both erythrocytes and megakaryocytes [80, 81, 91], its peak of expression in neutrophil precursors from human bone marrow [84] and its ability to either activate transcription [86,89] or mediate transcriptional repression [79], including in MCs [82], data suggest possible cooperation between F3 element overlapping *NRAMP1* exon XV and F10 candidate alternative TSSs located in intron 12. As a result, full-length transcription of *NRAMP1* may be prevented in myeloid cell types that either represent early progenitors of microbicidal phagocytes (i.e., MNs, PMNs and PM eosinophils) or diverge toward different lineages (e.g., erythrocytic/megakaryocytic) or various cell types such as DC and MC.

The suspected *NRAMP1* alternative TSS was also detected in larger CAGE datasets: it is the sole cluster of tags detected in ENCODE CAGE dataset (82 samples, including K562 cells but no other myeloid sample) [92] while it is apparently absent from two other sets that contain data from the monocytic lineage: (FANTOM3: 120 samples representing various human tissues, hence expected to contain resident populations of macrophages, including lung which is a major site of *NRAMP1* expression, [112]) [94] and (FANTOM4: THP1 CAGE, 36 samples including both untreated and phorbol-ester stimulated cells) [93]; and it was found in FANTOM5 (1829 sample-set that includes BloodCAGE data presented in Figure 1 and Figures S3-S7) [16,17].

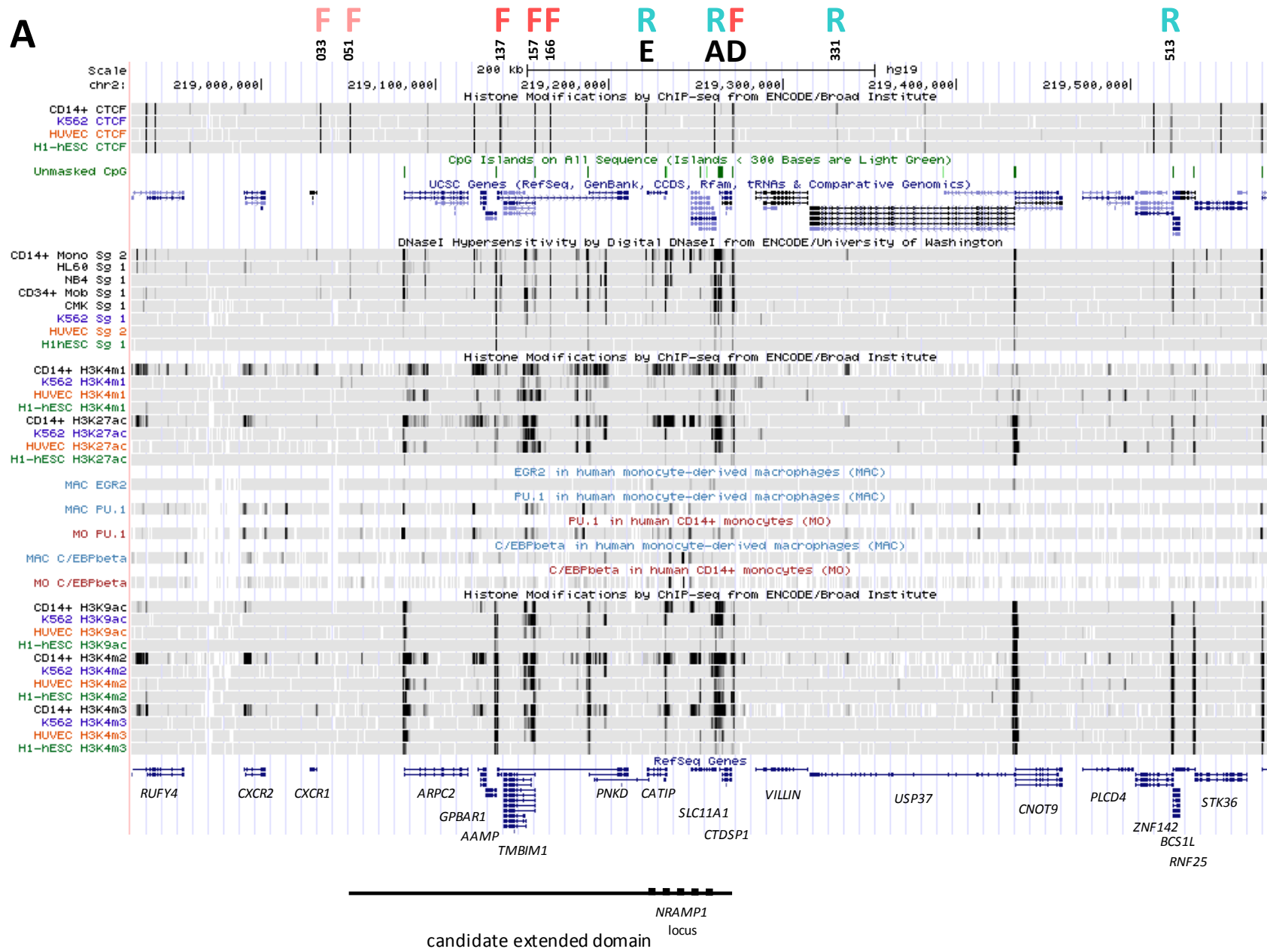
Further examination of *NRAMP1* expression data in THP1 monocytic cells (FANTOM4) shows that the gene is transcribed at low level in untreated cells. Gene expression is significantly induced after 24h treatment with phorbol-ester, to a level that is maintained slightly increased after 96h. These data confirm previous results obtained with HL-60 cells showing that *NRAMP1* expression is not induced rapidly during macrophage-like differentiation stimulated with phorbol ester (maximal induction attained after 48h treatment; [74]). In addition, examination of *NRAMP1* transcript level after siRNA perturbation against 53 TFs showed an up-regulation trend (twofold or more) in three instances: CTCF, IRF7 and MYC, suggesting that these factors may interfere with *NRAMP1* expression [93]. However since transcript expression was probed using the last exon (XV) the nature of the TSS involved (5' or "3' alternate") is not known.

Lastly, ChIP-seq data from untreated THP1 cells [93] associated the TFs SP1 and PU.1 with both the 5' and 3' parts of *NRAMP1* Orf, in agreement with other results implicating SP1 in *NRAMP1* expression in VitD-differentiated HL-60 cells [12] and demonstrating PU.1 binding at *NRAMP1* locus both in MNs and MDMs [13], whereas K9ac mark and RNA Pol II were found spread along *NRAMP1* locus including the 5' enhancer determinants. The negative element suspected in *NRAMP1* intron 12 (F10) corresponds to a peak in all four

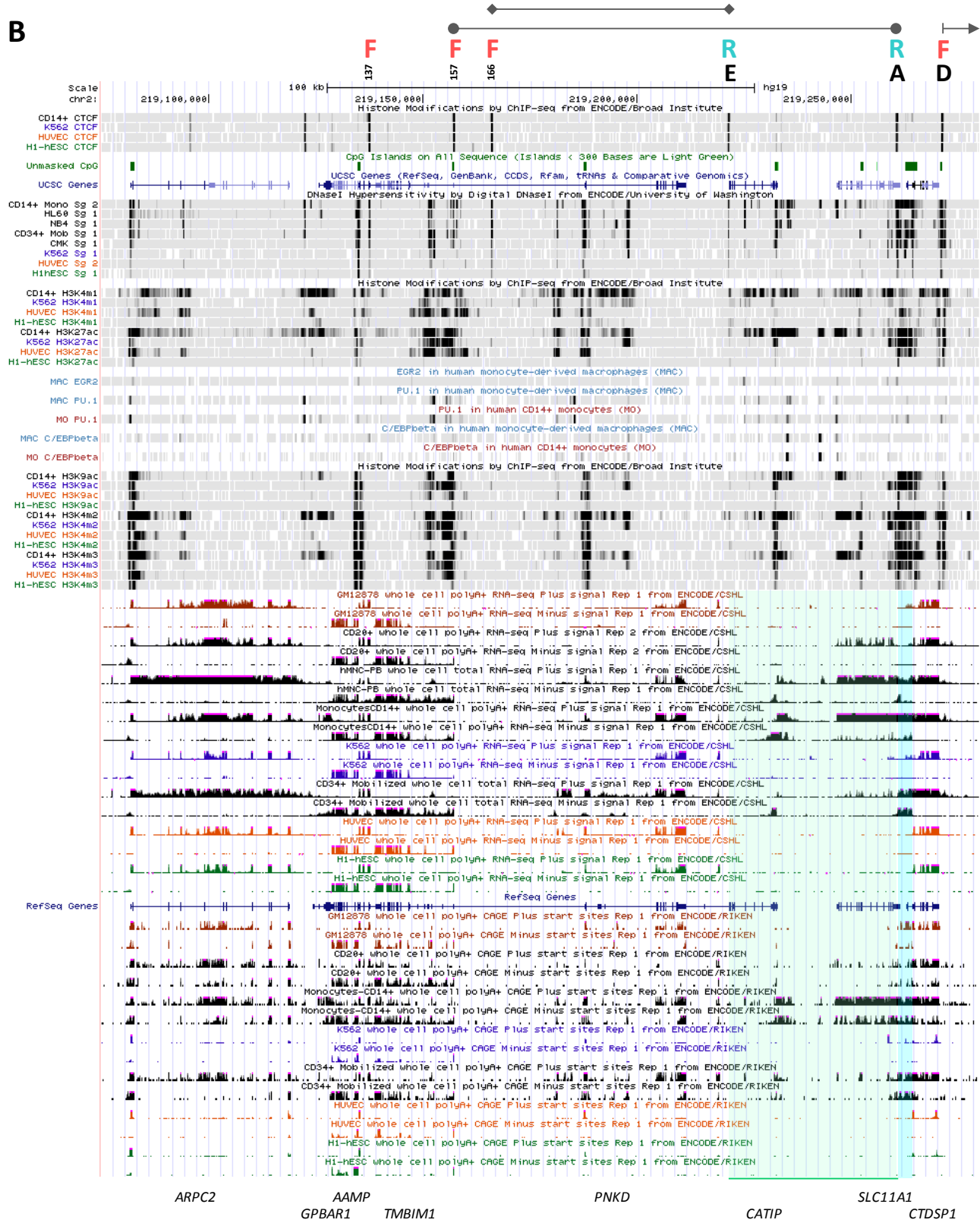
ChIP-seq analyses, which is more prominent in the case of SP1 compared to PU.1. In contrast, CAGE tags were few at this site while tag clustering at *NRAMP1* TSS was comparatively inferior to *CTDSP1* TSS, consistent with low level *NRAMP1* expression in untreated THP1 cells.

Legend to Figures S1-S28

Figure S1. CTCF-dependent topological organization of *NRAMP1* locus. **A.** View of a 700 kb chromosome 2 segment centered on *NRAMP1* (*SLC11A1*) gene [9, 10, 48, 78]. *From top to bottom:* Orientation of CTCF sites identified by ENCODE project, forward (F) and reverse (R), and labelled with numbers or letters; Chromosome 2 scale; CTCF ChIP-seq data from CD14⁺ MNs, K562, HUVEC and ESC; CpG islands; UCSC gene descriptions; DHS mapped in CD14⁺ MN, HL-60, NB4, G-CSF mobilized CD34⁺ precursors (mCD34/CMP), CMK, K562, HUVEC and ESC; Histone marks of activation (K4me1 and K27ac) in CD14⁺ MNs, K562, HUVEC and ESC; ChIP-seq data for EGR2 (MF/MAC), PU.1 and C/EBPb (MAC and MN/MO; [13]); Histone marks of transcriptional activity (K9ac, K4me2, K4me3) in CD14⁺ MN, K562, HUVEC and ESC; RefSeq gene descriptions. A candidate super-domain encompassing *NRAMP1* locus is indicated by a thick black line. **B.** Close-up view of CTCF-dependent looping around *NRAMP1* locus. *From top to bottom:* CTCF-dependent loops revealed by ChIA-PET analyses in both K562 and MCF7 cells; Orientation of the corresponding CTCF sites, F or R, identified by their genomic location; Chromosome 2 scale; CTCF ChIP-seq data from CD14⁺ MN, K562, HUVEC and ESC; CpG islands; UCSC gene descriptions; DHS mapped in CD14⁺ MN, HL-60, NB4, mCD34, CMK, K562, HUVEC and ESC; Histone marks of activation (K4me1 and K27ac) in CD14⁺ MN, K562, HUVEC and ESC; ChIP-seq data for EGR2 (MF), PU.1 and C/EBPb (MF and MN); Histone marks of transcriptional activity (K9ac, K4me2, K4me3) in CD14⁺ MN, K562, HUVEC and ESC; RNA-seq data for both strands from GM12878 lymphoblasts, CD20⁺ B lymphocytes, mononuclear cells from peripheral blood, CD14⁺ MN, K562, mCD34, HUVEC and ESC; RefSeq gene descriptions; whole cell CAGE for both strands from GM12878 lymphoblasts, CD20⁺ B lymphocytes, CD14⁺ MN, K562, mCD34, HUVEC and ESC. Green highlighting underlines myelo-monocytic specific transcription that typifies *NRAMP1* locus; a small contiguous area (blue highlight) delineates hematopoietic-specific transcription signals. **C.** Sequence of CTCF sites. Top: CTCF consensus sequence from various sources: JASPAR TF database [63], Factorbook database [61] and Guo *et al.* study [58]; Bottom: sequence and orientation of CTCF sites identified by ENCODE around *NRAMP1*; the three most conserved positions are underlined; # refers to CTCF site labels in panel A. **D.** Both *NRAMP1* locus CTCF boundaries comprise predicted eQTLs [54]. **a.** Immunopop server [54] display of 416 local eQTLs associated with *NRAMP1*, based on gene expression level variations measured in M2 MF/immature DC (CD14⁺, CD1a⁺, CD83^{low}, HLA-DR^{low}), either resting or infected for two hours with *Listeria* or *Salmonella*, from individuals of European and/or African ancestry. **b.** Blow-up of *NRAMP1* locus area (~70kb) highlighting the location of two SNPs widely used for *NRAMP1* genotyping which were previously associated with susceptibility to infectious diseases, including tuberculosis, and/or autoimmune pathologies (e.g., inflammatory bowel disease, rheumatoid arthritis [111]). Horizontal green arrows indicate eQTL haplotypes that were co-detected in independent studies [54,50]; the corresponding individual eQTLs are pointed with green arrowheads. **c.** UCSC genome browser display of the CTCF topologically associating domain (TAD) delineating *NRAMP1* locus. *From top to bottom:* Chromosome 2 scale; CTCF binding sites revealed by ChIP-seq assays in CD14⁺ MNs and K562 cells; CpG islands; RefSeq genes; DHS in CD14⁺ MN (x2); ENCODE TF binding sites detected by ChIP-seq assays; UCSC genes; Chromosome 2 regions (i-v) part of *NRAMP1* locus (CTCF TAD) carrying sets of transcriptional regulatory elements (F1-F14) predicted to control gene expression.



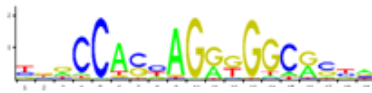
B



C

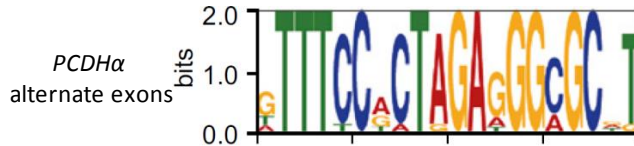
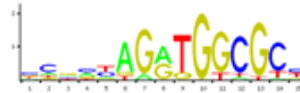
CTCF consensus sites:

JASPAR
(MA0139.1)



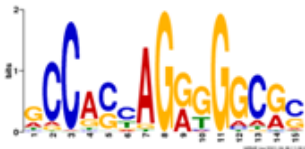
Mathelier, Fornes, Arenillas, Chen *et al.*, 2016

(MA0531.1)



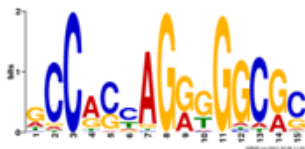
Guo, Monahan, Wu *et al.*, 2012

Factorbook
K562

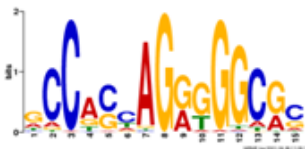


Wang, Zhuang, Iyer, Lin, Whitfield *et al.*, 2012

HUVEC



ESC



CTCF sites around *NRAMP1* locus:

	#	Strand	Orientation
GCCACAAGGGGGCAG	033	+	F
TCCAGGAGAGGGCAG	051	+	F
TCCACCAGAGGGCGC	137	+	F
GCCGCCAGGGGGCGC	157	+	F
ACCCTAGGGGGCAG	166	+	F
TCCAGCAGAGGGAGC	E	-	R
GCCCTAGGGGGAGC	A	-	R
GCCCTAGAGGCCTC	D	+	F
AACAGTAGGTGTAC	331	-	R
CCCACAAGAGGGTGC	513	-	R

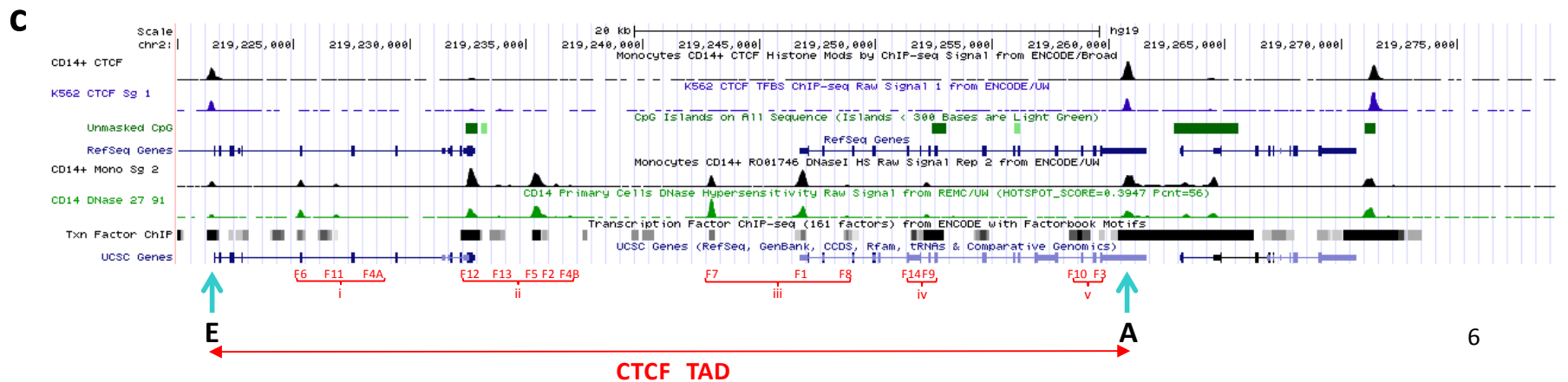
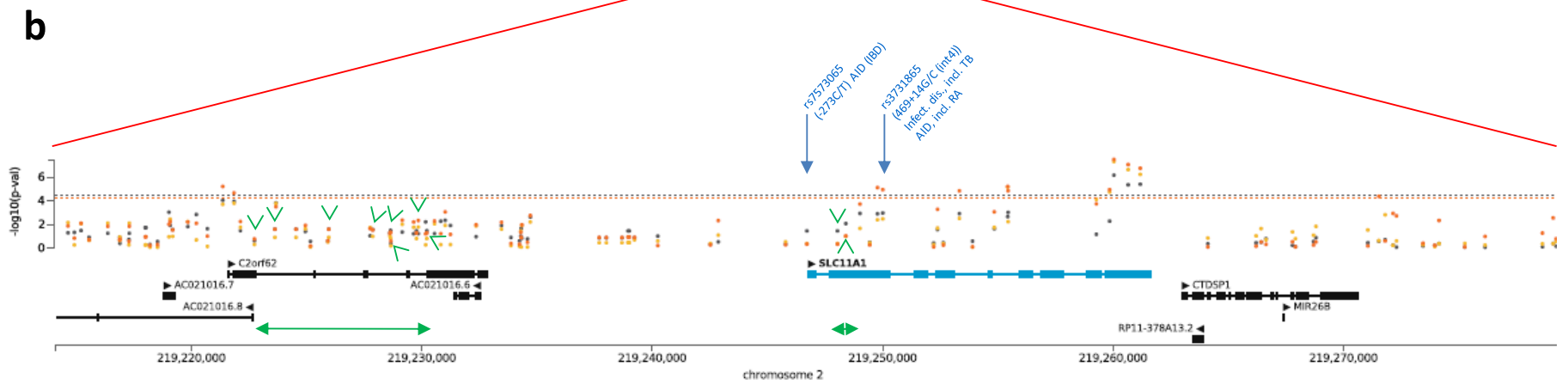
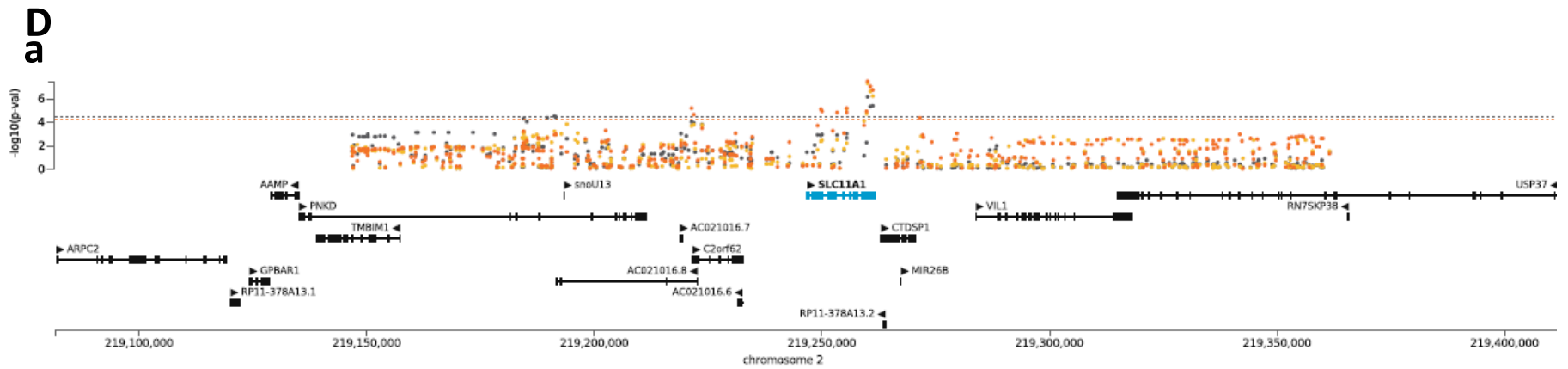


Figure S2. Regulatory element in *NRAMP1* intron 12 having negative impact on gene expression. **A.** Cap analysis of gene expression (CAGE) at *NRAMP1* locus showing the transcription start sites (TSS) of *NRAMP1* and downstream gene *CTDSP1* whereas the upstream gene *CATIP* is not expressed in myeloid cells [68]. CAGE for representative examples of cell types that express *NRAMP1* at high level (neutrophils, CD14⁺ MNs), at moderate level similar to *CTDSP1* (CD34⁺ progenitors, dendritic cells) or that show negligible *NRAMP1* expression (acute myeloid leukemias, mast cells). The mean of tags per million (tpm) detected over the 50kb analyzed is given for each cell type to illustrate the predominance of *NRAMP1* expression in mature phagocytes. A vertical arrow indicates a putative *NRAMP1* internal TSS that is detected in cells producing little full-length transcript.



Figure S2B. (Epi)genetic analysis of the 3' end of *NRAMP1* gene (exons XIII-XV) including ChIP-seq data for specific TFs and select histone marks, and DNase 1 footprints. *From top to bottom:* F10 and F3 denote DNase 1 footprints previously described [11]; chromosome 2 scale; ENCODE ChIP-seq for CTCF (CD14⁺ MNs, K562 cells), UCSC browser description of *NRAMP1* structure; CpG islands; ENCODE ChIP-seq data for various TFs; footprints of areas sensitive to DNase1 digestion (CD14⁺ MNs, HL-60 and NB4 cells, mCD34, CMK and K562 cells); ChIP-seq data for select histone marks of regulatory element priming (K4me1, K27ac; CD14⁺ MNs, K562 cells); ChIP-seq data for the TFs EGR2, PU.1 and C/EBPβ in MO and MAC [13]; ChIP-seq data for select histone marks of transcriptional activation (K9ac, K4me2, K4me3) in CD14⁺ MNs and K562 cells; RefSeq description of *NRAMP1* structure.

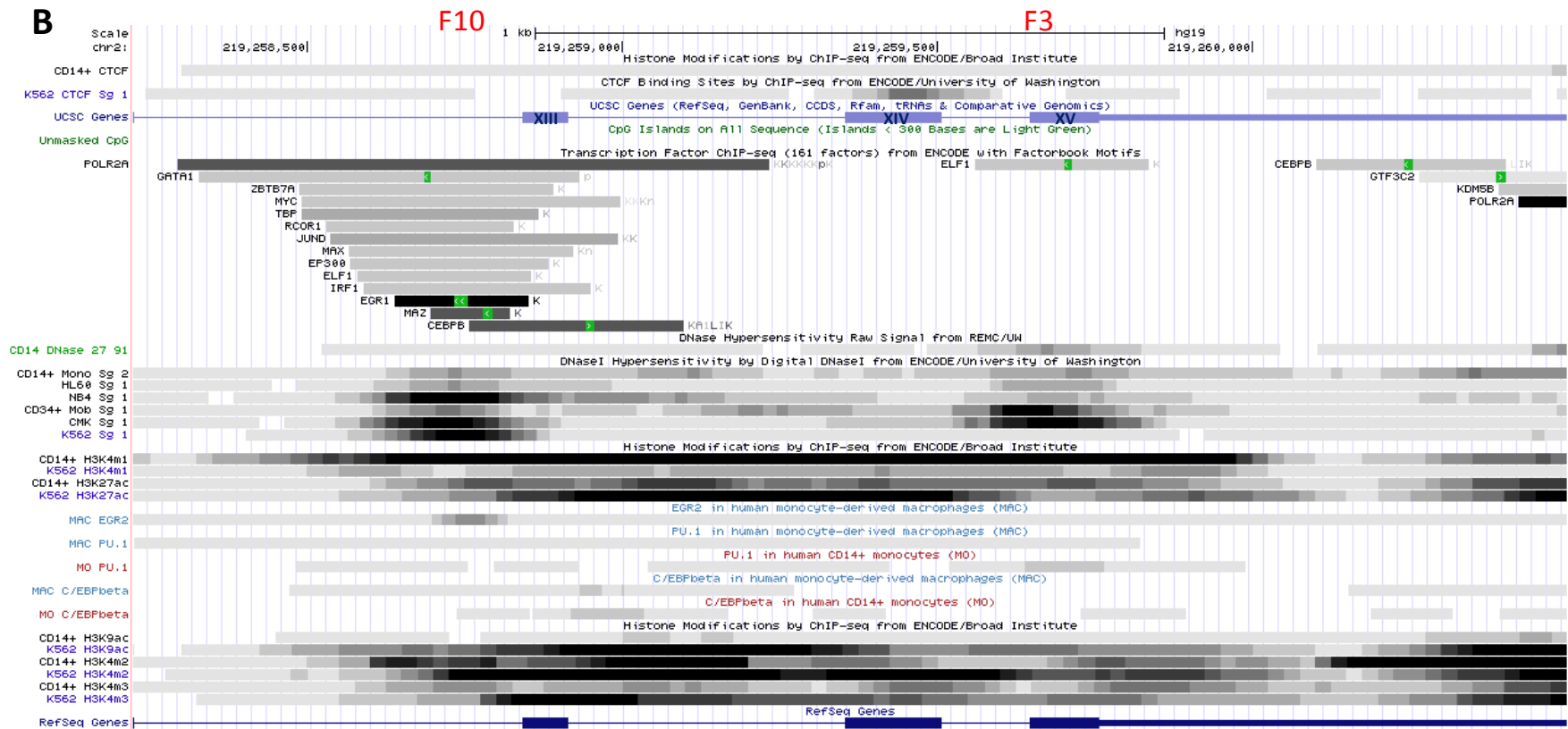


Figure S3. Detail of CAGE at *NRAMP1* region ii spanning DNase1 footprints (DHS) F12, F13, F5, F2 and F4B. *From top to bottom:* Location of DNase1 footprints (DHS, ENCODE); chromosome 2 scale; ENCODE CTCF ChIP-seq data for CD14⁺ MNs, HL-60, NB4 and K562 cells, HUVEC and ESC; CpG islands; DNase1 footprints in CD14⁺ MNs; UCSC browser gene descriptions; RNA Pol II ChIP-seq data for HL-60, NB4, K562, HUVEC and ESC; RefSeq genes; CAGE data for 22 blood cell types [68].



Figure S4. Detail of CAGE at *NRAMP1* region iii spanning DNaseI footprints (DHS) F7, F1 (TSS) and F8. *From top to bottom:* same as Figure S2.

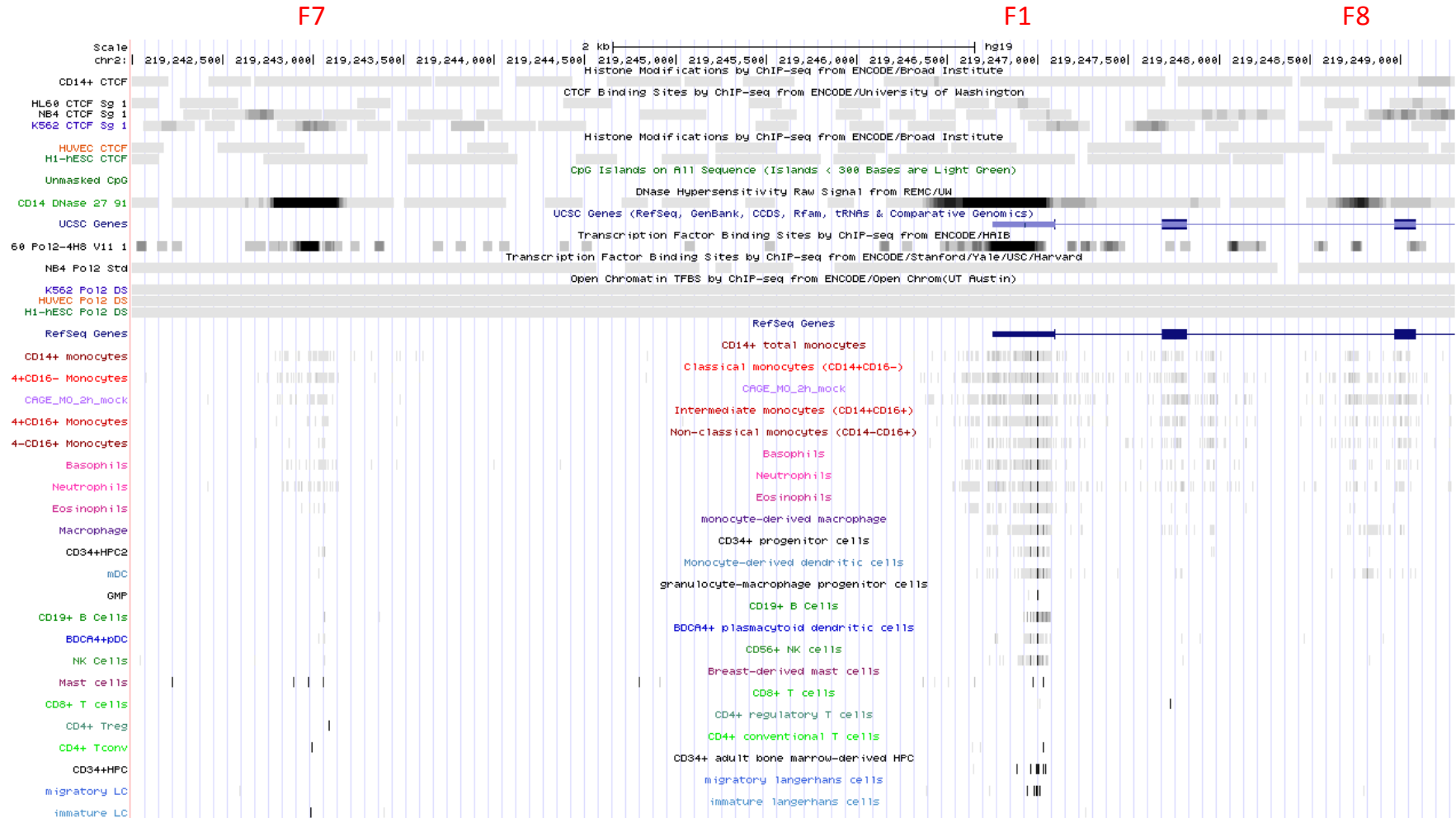


Figure S5. Detail of CAGE at *NRAMP1* region i spanning DNase1 footprints (DHS) F6, F11 and F4A. *From top to bottom:* same as Figure S2.

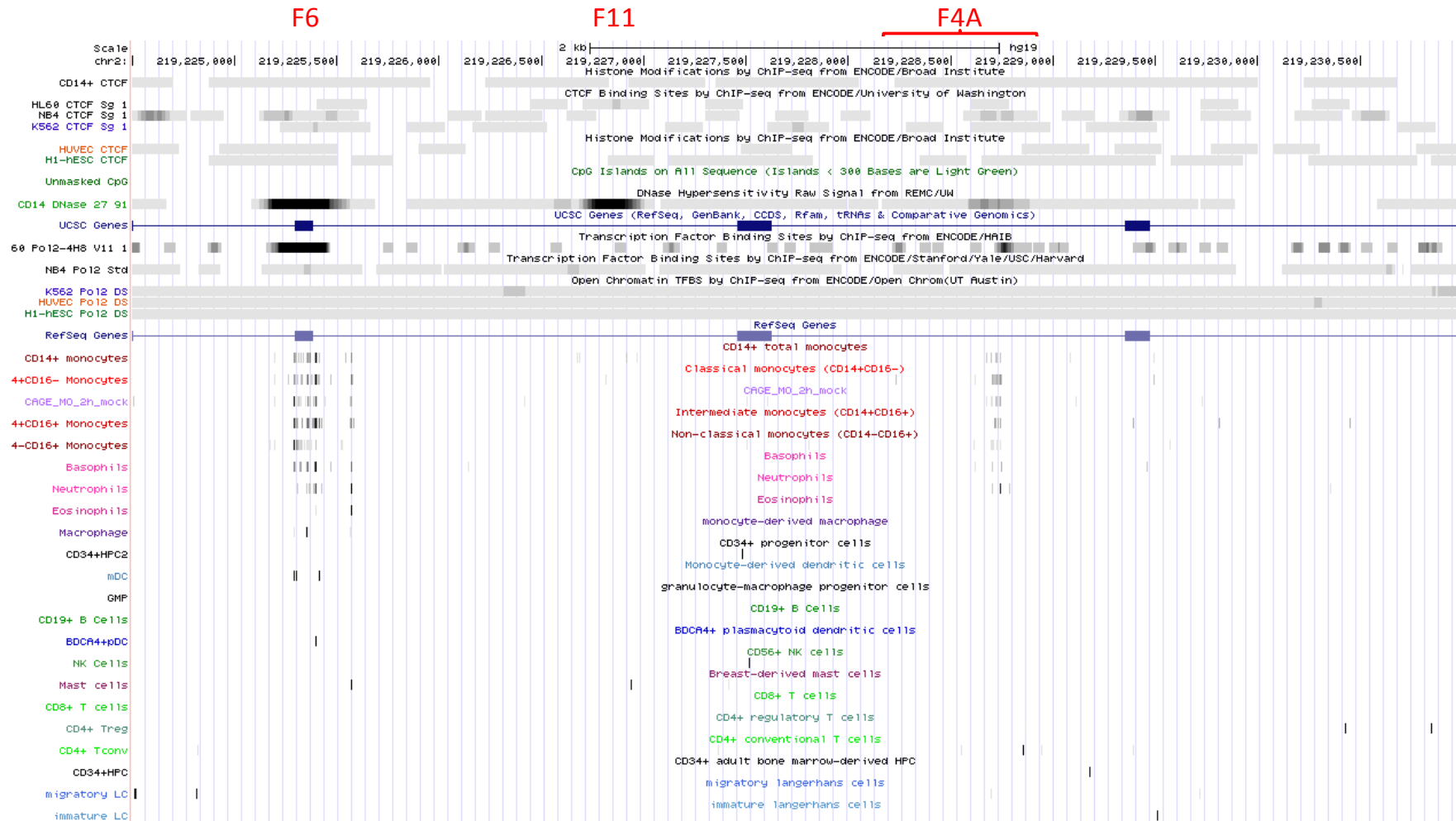


Figure S6. Detail of CAGE at *NRAMP1* region iv spanning DNase1 footprints (DHS) F14 and F9. *From top to bottom:* same as Figure S2.

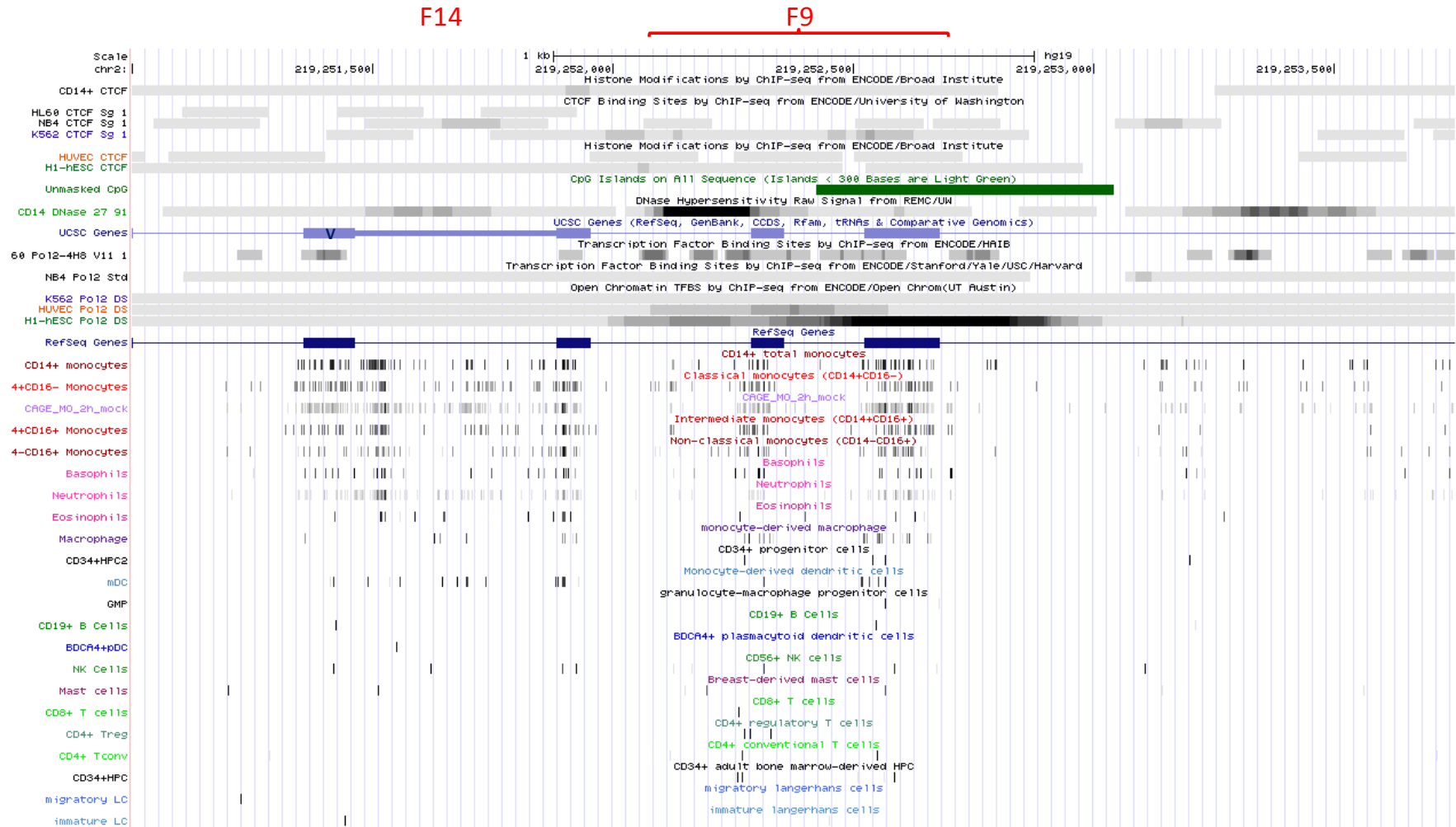


Figure S7. Detail of CAGE at *NRAMP1* region v spanning DNase1 footprints (DHS) F10 and F3. From top to bottom: same as Figure S2.

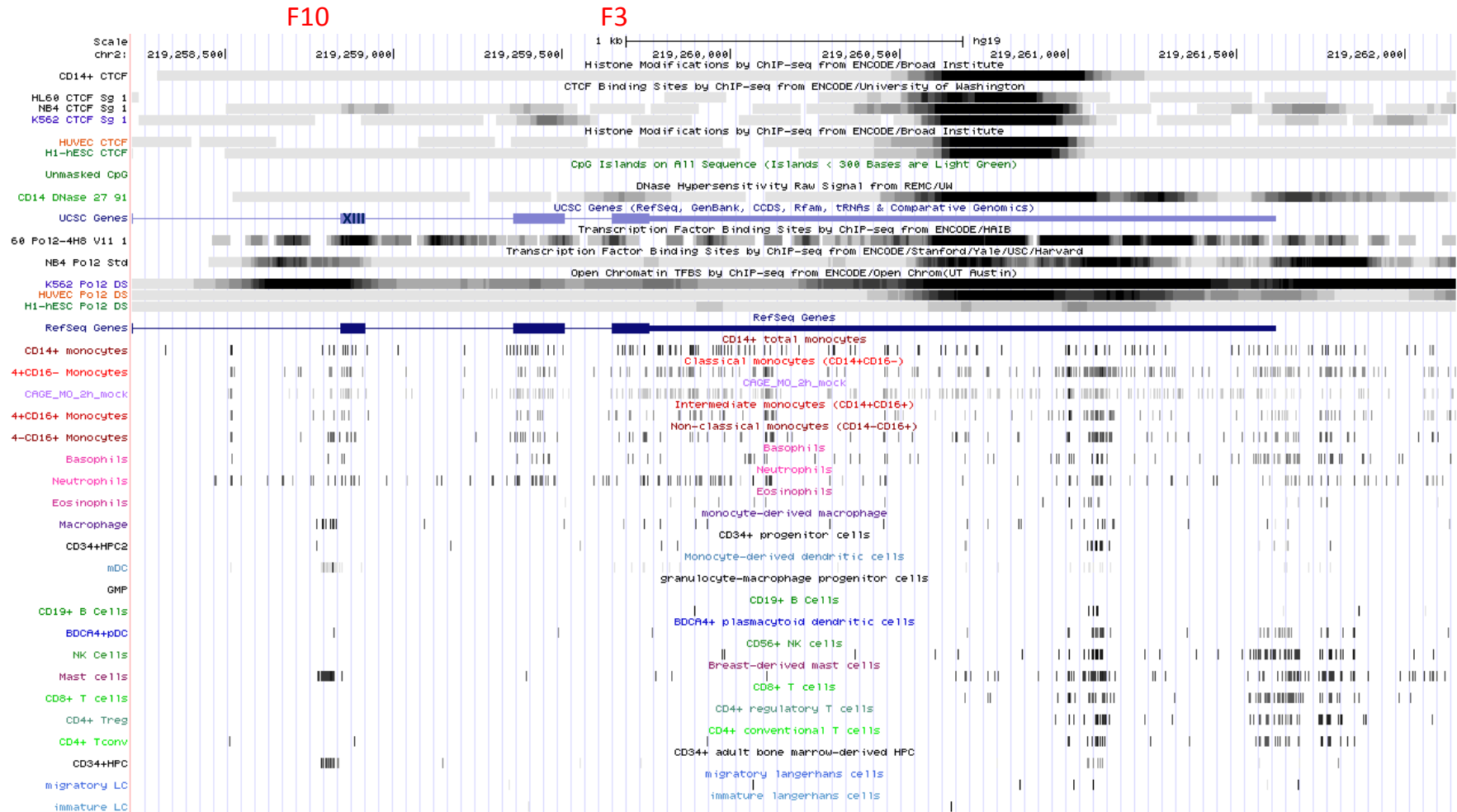


Figure S8. ChIP-seq data for histone marks of de-activation: K27me3 (transcriptionally silent chromatin) and K9me3 (heterochromatin). *NRAMP1* locus is examined at two different scales: **upper panel**, 6Mb, a vertical arrow localizes the gene; **lower panel**, 55kb, the gene is underlined. For each panel, *from top to bottom*: chromosome 2 banding pattern; local chromosome 2 scale; CpG islands; ENCODE CTCF ChIP-seq data for ESC, HUVEC, CD14⁺ MNs and K562 cells; UCSC gene descriptions; DNase1 footprints for CD14⁺ MNs, HL-60 and NB4 cells, mCD34, CMK and K562 cells; ChIP-seq data for the TFs EGR2, PU.1 and C/EBPβ in MN and MF [13]; ChIP-seq data for select histone marks of chromatin de-activation (K27me3 and K9me3; ESC, HUVEC, CD14⁺ MNs and K562 cells); RefSeq gene descriptions.

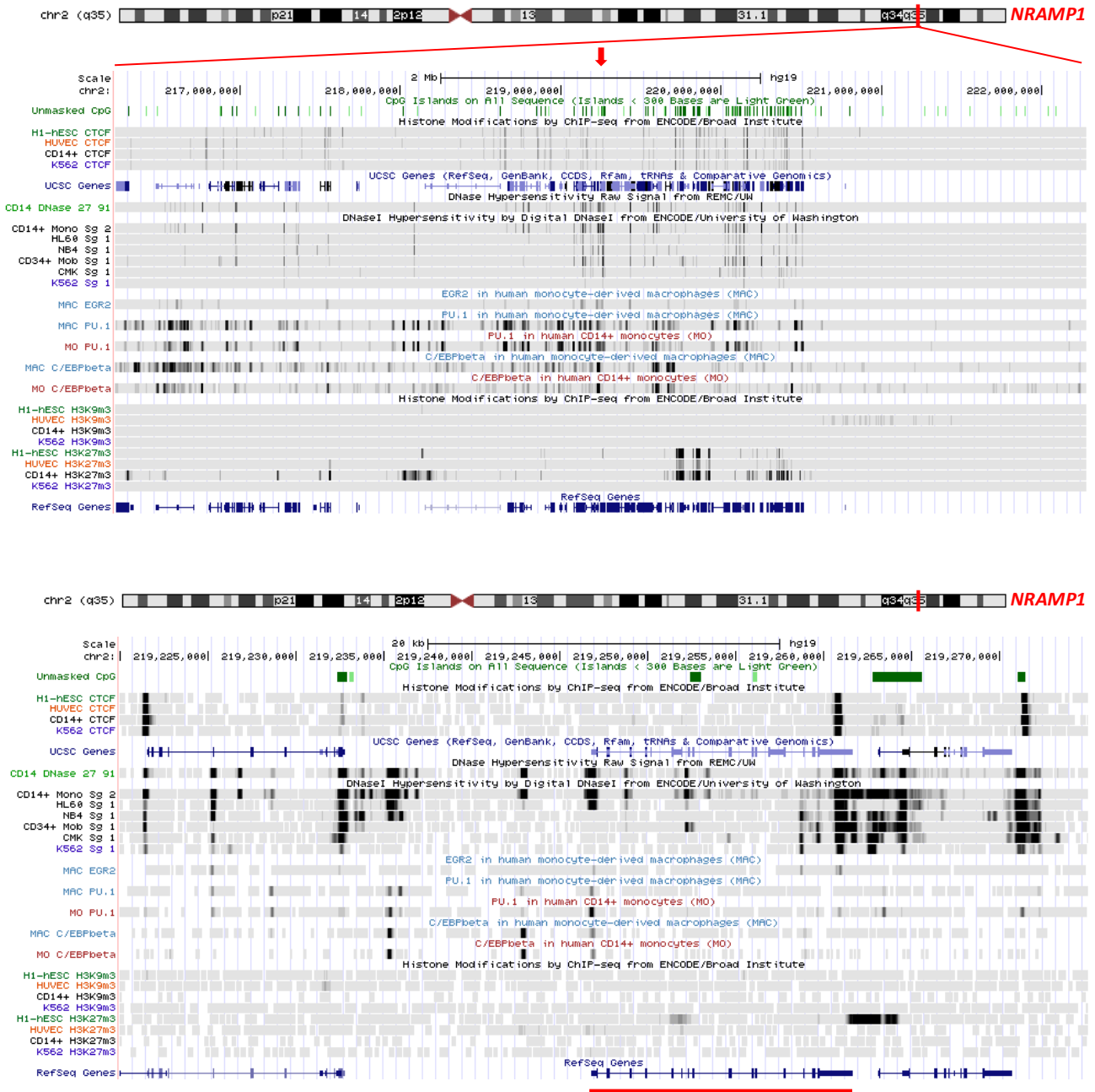


Figure S9. UCSC browser display of ENCODE TF-specific ChIP-seq data for *NRAMP1* locus shows TF association with multiple DHS, including several CTCF sites. *From top to bottom:* position and orientation of CTCF sites, indicated by colored letters: red (forward), blue (reverse) and grey (undetermined); chromosome 2 scale bar; CD14⁺ MN DHS; CTCF-specific ChIP-seq (K562 cells); UCSC gene descriptions; CpG Islands; ENCODE TF-specific ChIP-seq data shows variable enrichment at CTCF sites; CTCF-specific ChIP-seq (CD14⁺ MNs); CD14⁺ MN DHS; Refseq gene descriptions.



Figure S10. Association of TF mediating inflammatory responses with *NRAMP1* locus. *From top to bottom:* major CTCF binding sites E, A and D; gene names and position of *NRAMP1* TSS; chromosome 2 regions carrying predicted transcriptional regulatory elements (F1-F14); chromosome 2 scale; IRF1 ChIP-seq data for MDM (in presence of M-CSF), stimulated for 6h with or without LPS and with or without 24h IFN-g priming [99]; Other RefSeq gene descriptions; STAT1 ChIP-seq data for MDM stimulated for 6h with or without LPS and with or without 24h IFN-g priming [99]; UCSC gene descriptions; HIF1a and HIF2a association with *NRAMP1* locus in MDM (RPMI medium alone) exposed to hypoxia for 4h at 37°C after priming or not with IL-10 for 16h [103]; Basic gene depictions; ChIP-seq for EGR2 (MF), C/EBP β and PU.1 (MN and MF) [13]; Ensembl Genes; ENCODE DHS for CD14⁺ MNs, HL-60, NB4, K562 and CMK cells, mCD34, CD34⁺ progenitors; CTCF specific ChIP-seq in CD14⁺ MNs; K27ac specific ChIP-seq data for MN and MF [13], CD14⁺ CD16⁻ MNs and CD14⁻ CD16⁺ MNs [152], CD14⁺ MNs and CD34⁺ progenitors (ENCODE); CTCF specific ChIP-seq in ESC; K4me1 specific ChIP-seq data for MO and MAC [13], CD14⁺ MNs, CD34⁺ progenitors and HSC (ENCODE); CpG islands; K9ac ChIP-seq data (CD14⁺ MNs); CTCF specific ChIP-seq in K562 cells; K4me2 and me3 ChIP-seq (CD14⁺ MNs); RefSeq genes; ChIP-seq in CD14⁺ MNs (H4K20me1, K79me2, K36me3); CTCF specific ChIP-seq in HUVEC; CAGE data for CD14⁺ CD16⁻ MNs and CD14⁻ CD16⁺ MNs [152].

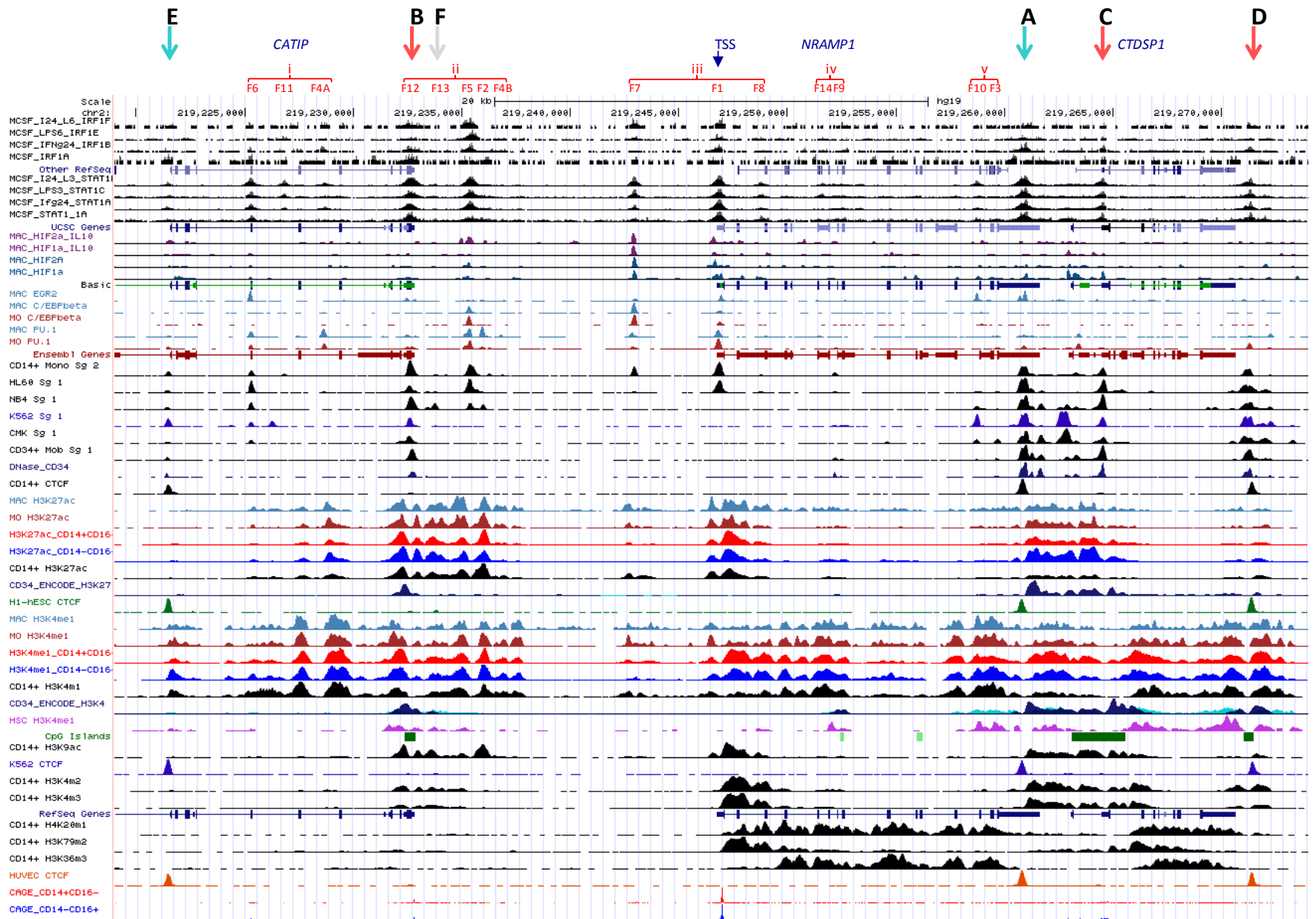


Figure S11. Predicted *NRAMP1* super-enhancer (S-E) determinant. *From top to bottom:* Chromosome 2 scale; ChIP-seq for CTCF (CD14⁺ MNs, K562 cells, ESC); CpG islands; UCSC gene description; DHS (CD14⁺ MNs, HL-60 and NB4 cells, mCD34, CMK and K562 cells); ChIP-seq data (K27ac, K4me1 and the TFs PU.1 and C/EBP β in MN and MF [13]; polyA⁺ CAGE tags for CD14⁺ MNs, mCD34, K562 cells, ESC [16,17]; RefSeq genes; dbSUPER prediction of S-E determinants in CD14⁺ MNs, K562 cells and CD34⁺ precursors [101]



Figure S12. Comparison of ChIP-seq data at *NRAMP1* locus for histone marks of chromatin activation (K4me1, K27ac and K4me3) from select cell types (ESCs, ESC-derived cultured cells) and various tissues of mesodermal origin [14]. Each panel is depicted using a common Y-scale. *NRAMP1* predicted 5' and 3' regulatory hubs (RH) are highlighted (red and brown, respectively).

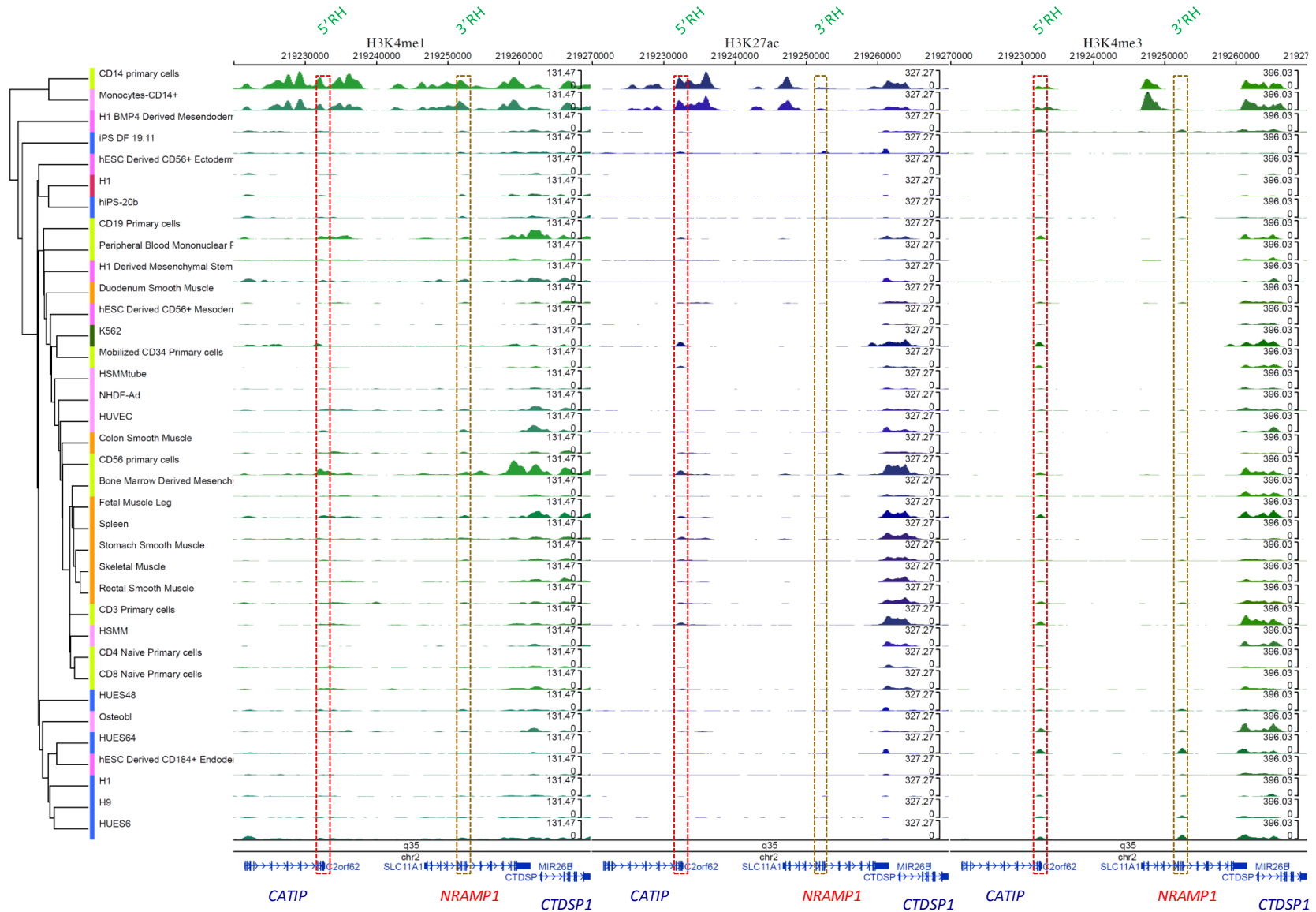


Figure S13. Comparison of ChIP-seq data at *NRAMP1* locus for histone marks of chromatin de-activation (K27me3 and K9me3) from select cell types (ESCs, ESC-derived cultured cells) and various tissues of mesodermal origin [14]. Each panel is depicted using a common Y-scale. *NRAMP1* predicted 5' and 3' regulatory hubs (RH) are highlighted (red and brown, respectively). K4me1 mark added for comparison with Figure S12.

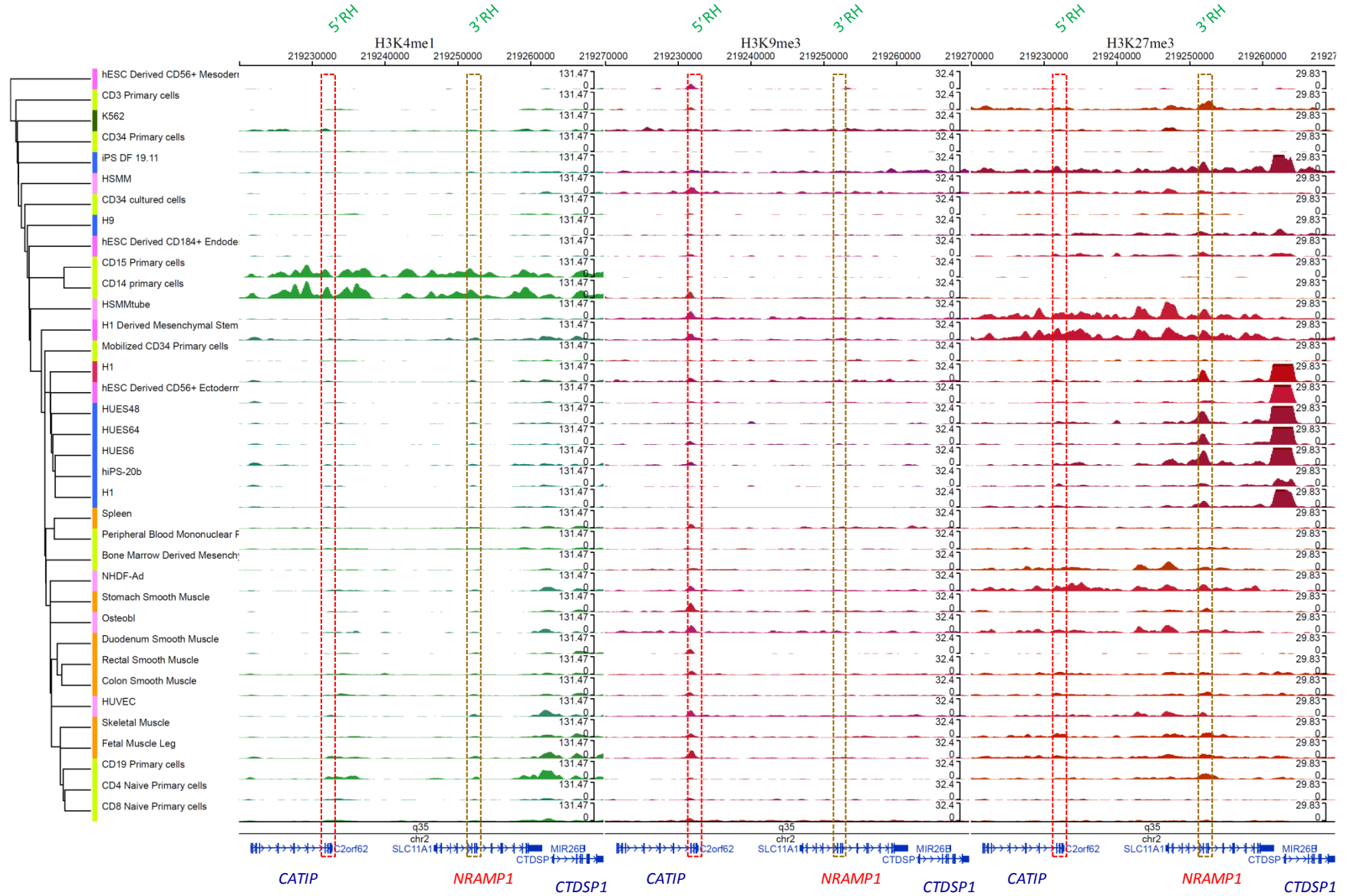


Figure S14. ENCODE CAGE and RNA-seq data corresponding to *NRAMP1* locus. Results are presented separately for five regions (i-v). *From top to bottom:* Location of DHSs; chromosome 2 scale; CTCF ChIP-seq for CD14⁺ MNs, K562 cells, HUVEC and ESC; CpG islands; UCSC gene description; DHSs in CD14⁺ MNs, HL-60, NB4, mCD34/CMP, CMK and K562 cells, HUVEC and ESC; ChIP-seq for histone marks of priming (K27ac, K4me1; CD14⁺ MNs, K562 cells, HUVECs and ESCs); ChIP-seq for the TFs PU.1 and C/EBP β in MN and MF; ChIP-seq for histone marks of activation (K9ac, K4me2 and K4me3); RNA-seq data (CD14⁺ MNs, K562 cells, mCD34, HUVEC and ESC); RefSeq gene description; CAGE data (CD14⁺ MNs, K562 cells, mCD34, HUVEC and ESC).



Region i



Region ii



Region iii

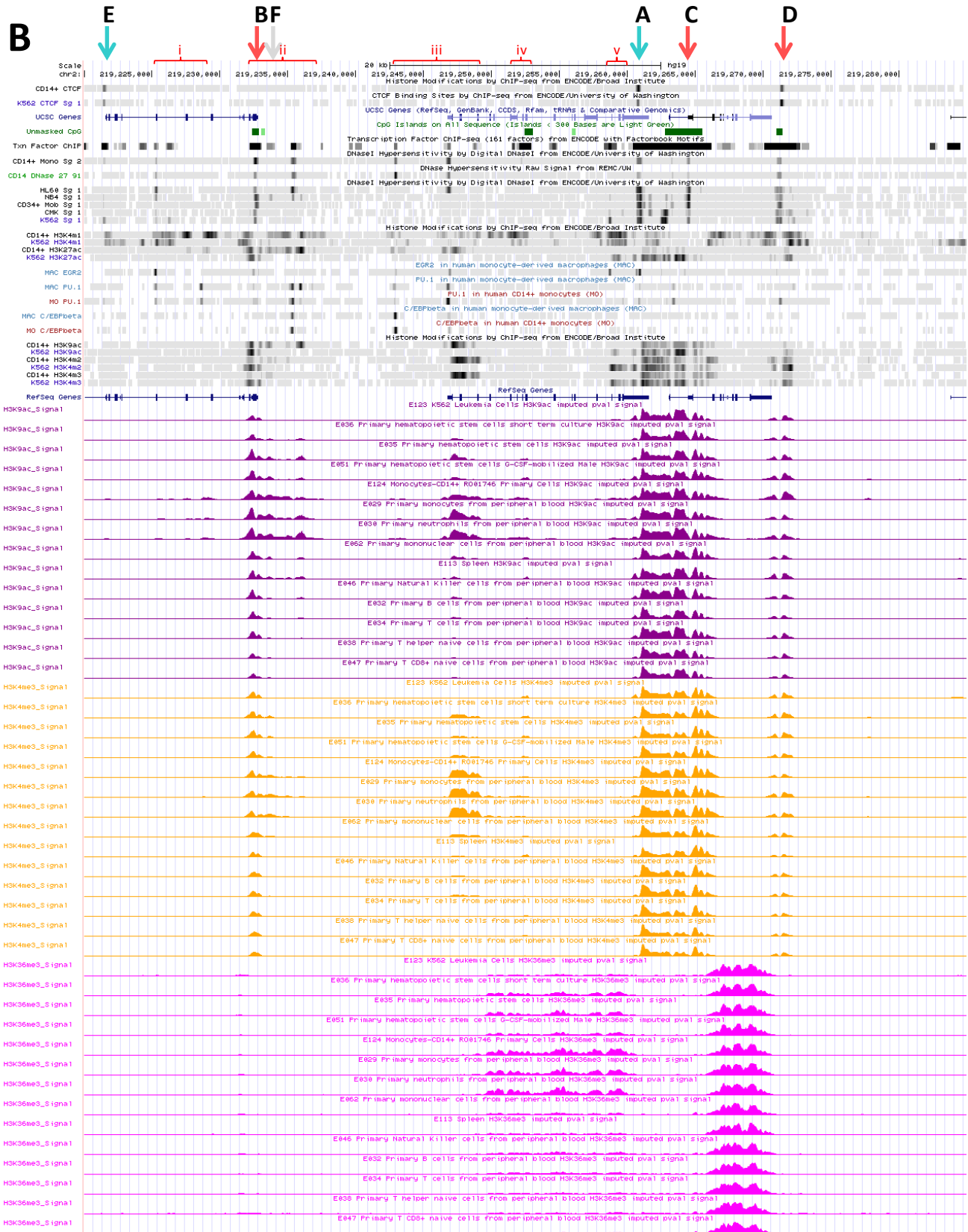


Region iv



Region v

Figure S15. Chromatin status at *NRAMP1* locus in hematopoietic cells. *From top to bottom:* position and orientation of CTCF sites indicated by arrows, red (forward), blue (reverse) and grey (undetermined); chromosome 2 regions carrying predicted transcriptional regulatory elements (F1-F14); chromosome 2 scale bar; ENCODE CTCF-specific ChIP-seq (CD14⁺ MNs, K562 cells); UCSC gene descriptions; CpG Islands; ENCODE TF-specific ChIP-seq data; ENCODE DHS for CD14⁺ MNs (x2), HL-60, NB4, mCD34, CMK and K562 cells; ENCODE ChIP-seq data for select histone marks (K4me1 and K27ac) in CD14⁺ MNs and K562 cells; ChIP-seq data for the TFs EGR2, PU.1 and C/EBP β in MO and MAC [13]; ENCODE ChIP-seq data for histone marks K9ac, K4me2 and K4me3 in CD14⁺ MNs and K562 cells; RefSeq gene descriptions; NIH Roadmap epigenomic data for hematopoietic cells: DHS and ChIP-seq data for histone marks of priming, K4me1 and K27ac (panel **A**); ChIP-seq data for histone marks of transcriptional activity, K9ac, K4me3 and K36me3 (panel **B**); RNA-seq profile and ChIP-seq data for histone marks of repression, K9me3 and K27me3 (panel **C**)



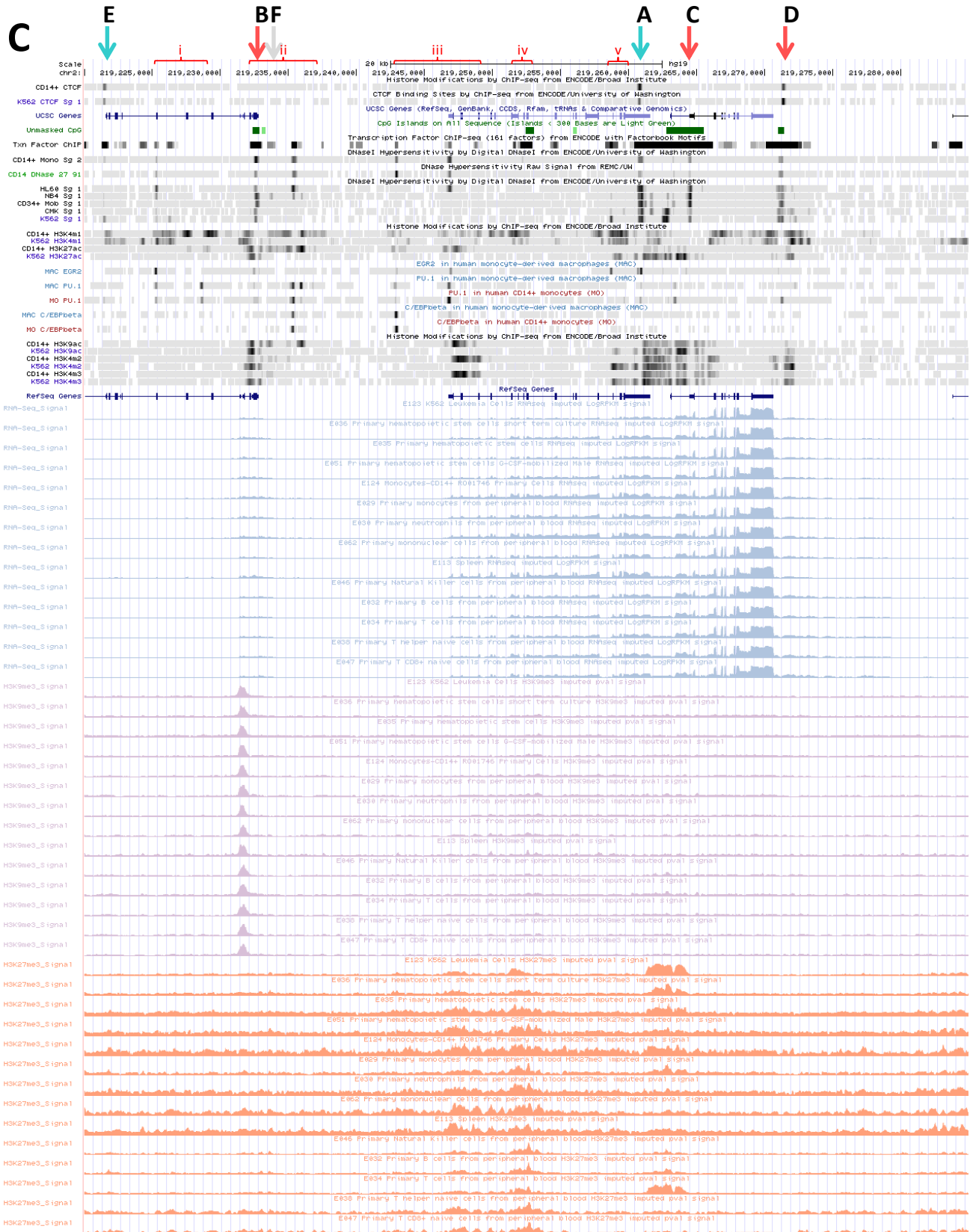
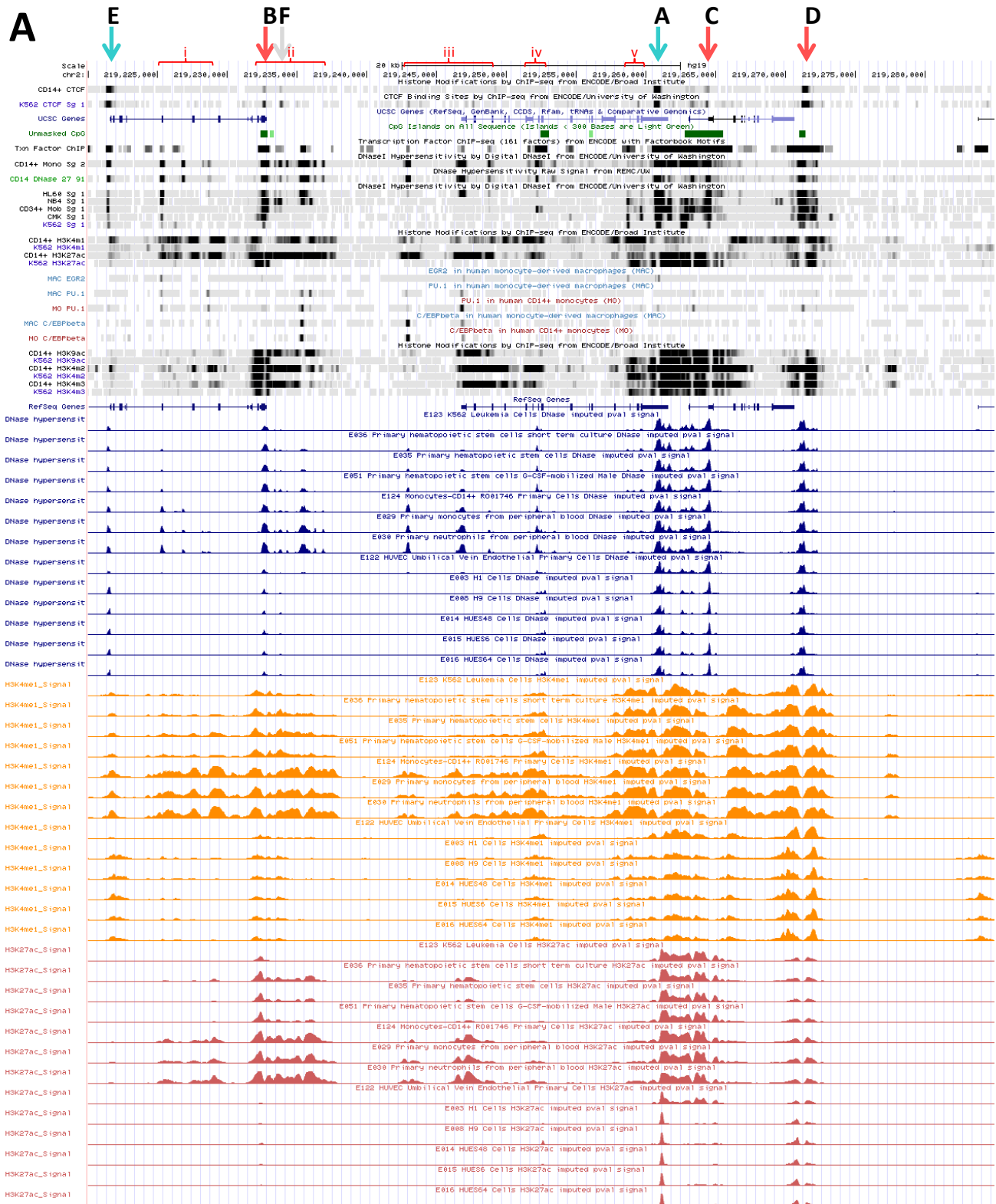


Figure S16. Chromatin status at *NRAMP1* locus in myeloid cells, HUVEC and ESC. *From top to bottom:* position and orientation of CTCF sites indicated by arrows, red (forward), blue (reverse) and grey (undetermined); chromosome 2 regions carrying predicted transcriptional regulatory elements (F1-F14); chromosome 2 scale bar; ENCODE CTCF-specific ChIP-seq (CD14⁺ MNs, K562 cells); UCSC gene descriptions; CpG Islands; ENCODE TF-specific ChIP-seq data; ENCODE DHS for CD14⁺ MNs (x2), HL-60, NB4, mCD34, CMK and K562 cells; ENCODE ChIP-seq data for select histone marks (K4me1 and K27ac) in CD14⁺ MNs and K562 cells; ChIP-seq data for the TFs EGR2, PU.1 and C/EBP β in MO and MAC [13]; ENCODE ChIP-seq data for histone marks K9ac, K4me2 and K4me3 in CD14⁺ MNs and K562 cells; RefSeq gene descriptions; NIH Roadmap epigenomic data for mesodermal cell types and ESCs: DHS and ChIP-seq data for histone marks of priming, K4me1 and K27ac (panel **A**); ChIP-seq data for histone marks of transcriptional activity, K9ac, K4me3 and K36me3 (panel **B**); RNA-seq profile and ChIP-seq data for histone marks of repression, K9me3 and K27me3 (panel **C**).



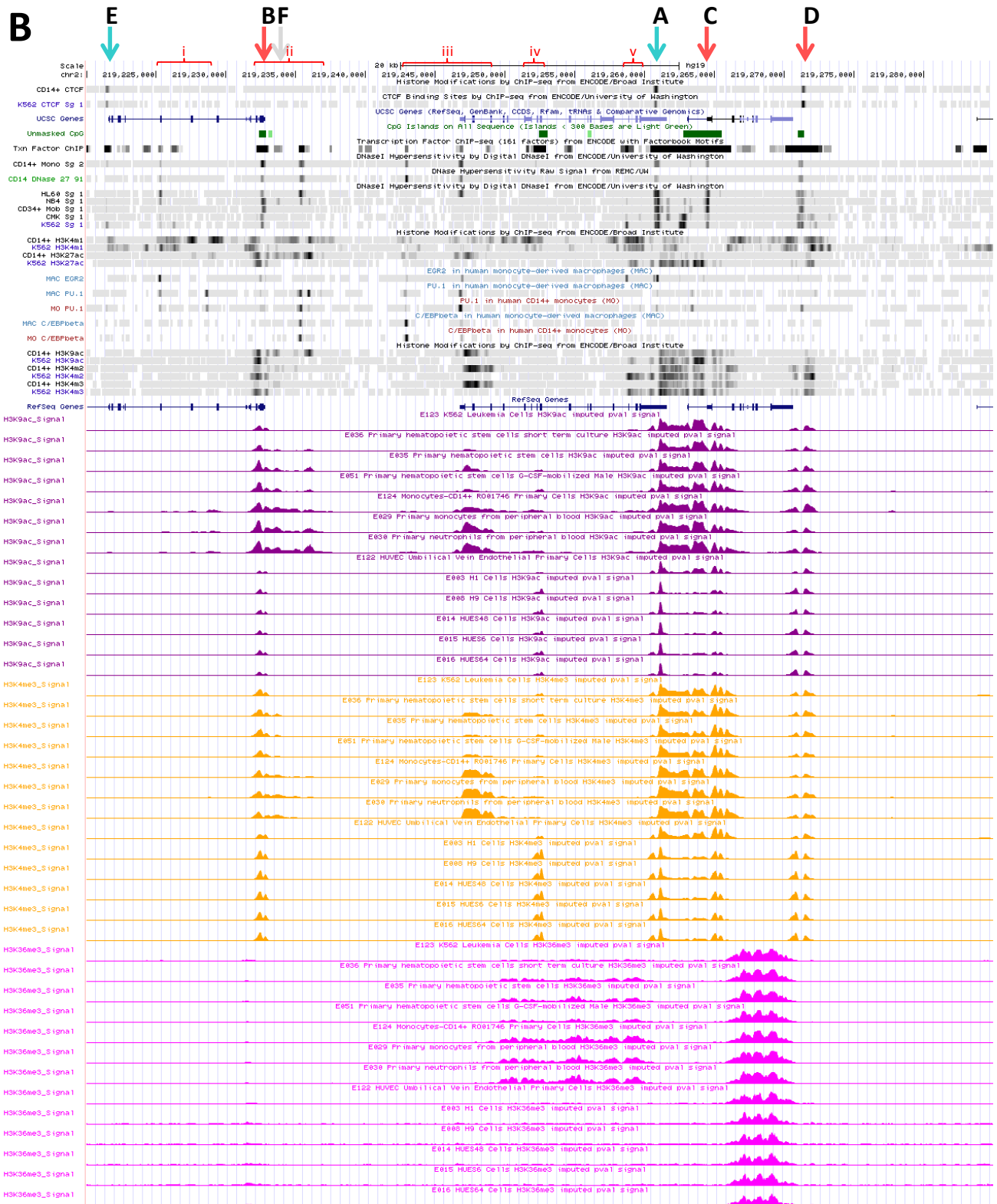




Figure S17. Hypothetical CTCF-dependent topology of *NRAMP1* locus and hematopoietic determinants of gene expression (see text for details, sections 2.3.3. and 2.3.4.). *NRAMP1* locus boundaries (CTCF sites A and E, "R" orientation, shown in black) are represented interacting with compatible and preferred upstream CTCF sites ("F" orientation, indicated as 157 and 166, respectively). Other CTCF sites are indicated in grey ("F" or undetermined orientation: B-D and F, respectively). DHS F1-F14 are colored depending on temporal order of mobilization: purple, light purple, pink and red. It is proposed that *NRAMP1* (*SLC11A1*) locus activation results from successive steps: i) F12/5'RH (CTCF_B) and F9/3'RH are partially mobilized in non-hematopoietic cell types; ii) initiation of hematopoiesis may erase negative histone marks leading to increased *CTDSP1* transcription -a process that may result from formation of a CTCF-dependent loop involving sites F and C (orange dotted arrow); iii) myeloid-specific TF-dependent mobilization of F12/5'RH, F13 and co-activation of sites F6, F10-F3 may prime the locus while preventing gene expression; iv) as differentiation progresses, specific myelomonocytic TFs activate elements F5, F7 and F9 leading to disruption of CTCF_F-C loop and allowing contacts between distal regulatory elements and NR1 TSS (F1), through Mediator based interactions for instance, which activate *NRAMP1* transcription (green dotted arrow); and v) terminal differentiation into mature phagocytes leads to extensive priming/activation of the locus, including elements F11, F4A, F2, F4B, F8 and F14, and further modulation by signal-dependent TFs (e.g., tissue microenvironment, infections...). According to this hypothesis, CTCF determinants define *NRAMP1* locus (TAD); hematopoietic TFs are required for transcriptional activation of the locus 3' end; myeloid TFs allow *NRAMP1* locus priming for subsequent activation while myelo-monocytic TFs mediate *NRAMP1* expression and/or signal-dependent regulation.

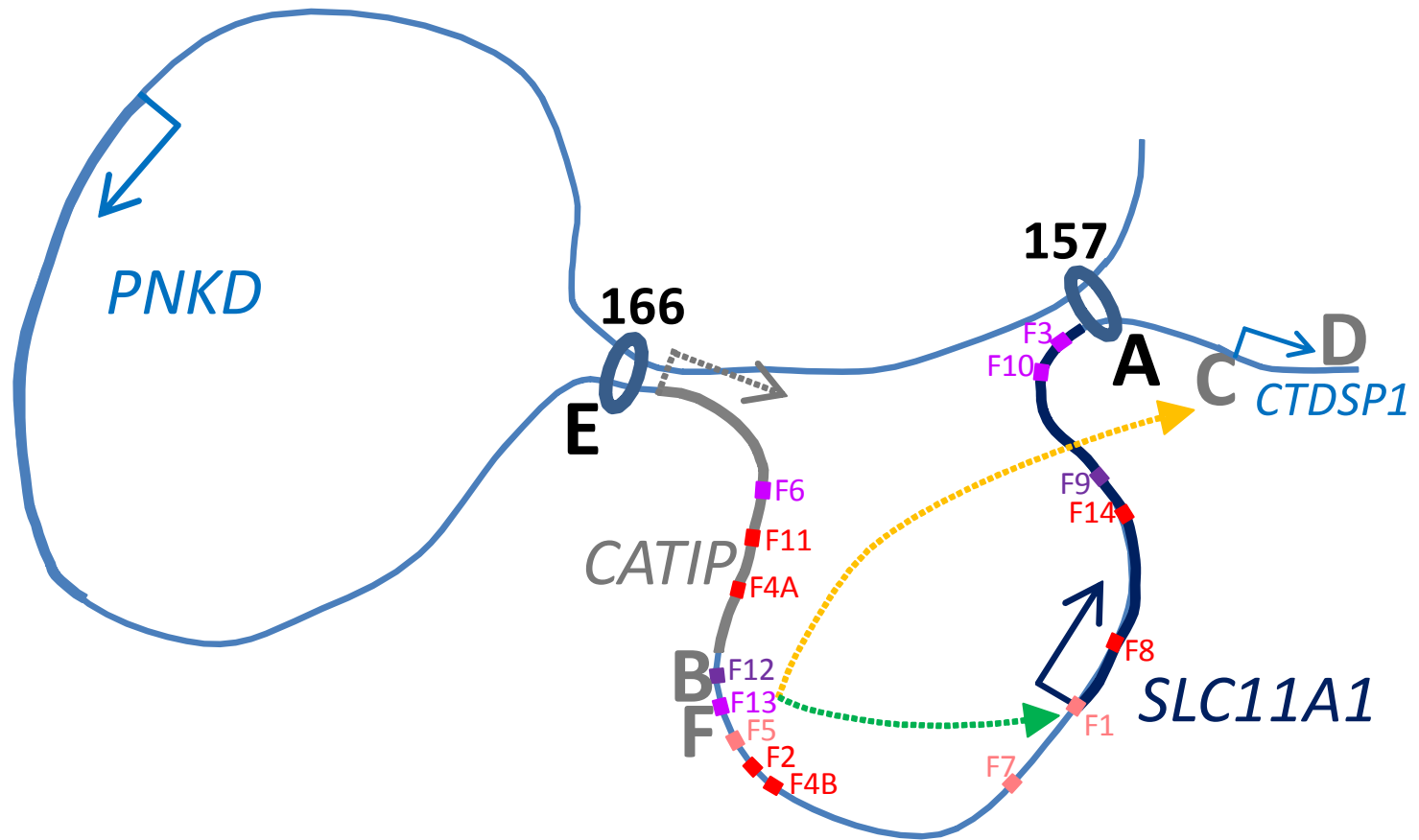


Figure S18. *NRAMP1* locus region i and ii represent candidate transcriptional regulatory determinants mediating innate memory in response to microbial stimuli from various origins (*Saccharomyces cerevisiae* $\beta(1,3)$ D-glucan, BG, and *Escherichia coli* lipopolysaccharide, LPS) [128]. From top to bottom: Major CTCF sites E, A and D (blue and red arrows correspond to reverse and forward orientations, respectively); gene names and position of *NRAMP1* TSS; candidate *NRAMP1* regulatory regions i-v, including DHS F1-F14; chromosome 2 scale; CpG islands; ENCODE CTCF-specific ChIP-seq data in CD14⁺ MNs; histone modification-specific ChIP-seq (K4me1, K27ac, K4me3) and Tn5 transposase accessibility (ATAC-seq) data for MNs stimulated with: a) LPS, for 24h and analyzed five days after (LPS_D6), b) BG, for 24h and analyzed five days after (BG_D6), c) no additive, for 24h and analyzed five days after (RPMI_D6), d) LPS, for 24h (LPS_D1), e) BG, for 24h (BG_D1) and f) no additive, for 24h (RPMI_D1), as well as for freshly explanted MNs (RPMI_0); ENCODE DHS (x2) and ChIP-seq analyses for similar histone modifications in CD14⁺ MNs (K4me1, K27ac, K4me3); UCSC genes; ChIP-seq data for the TFs EGR2, PU.1 and C/EBP β in MO and MAC [13]; ENCODE CTCF ChIP-seq data in K562 cells; ENCODE TF-specific ChIP-seq data; delineation of *NRAMP1* regions i-v.

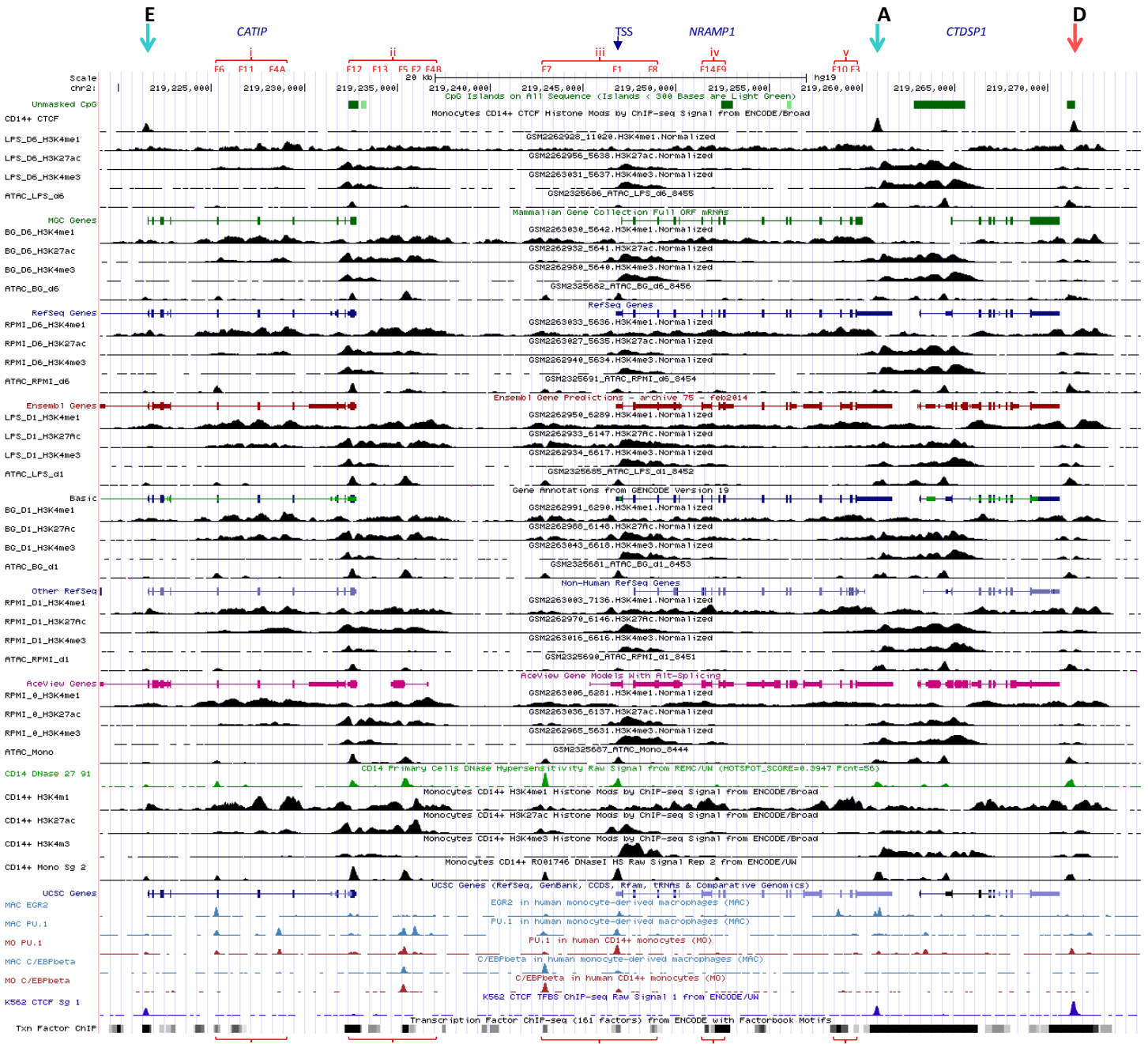


Figure S19. DHS and binding of RUNX1 at *NRAMP1* locus in FLT3-ITD AML patients [139]. From top to bottom: chromosome 2 scale; RefSeq gene descriptions; DHS in CD14⁺ MNs, CD34⁺ peripheral blood stem cells (PBSC), FLT3-ITD AMLs (x3) and MNs; RUNX1-specific ChIP-seq in CD34⁺ cells and FLT3-ITD AMLs (x2); DHS in HL-60 cells; GENCODE gene descriptions; CpG islands.

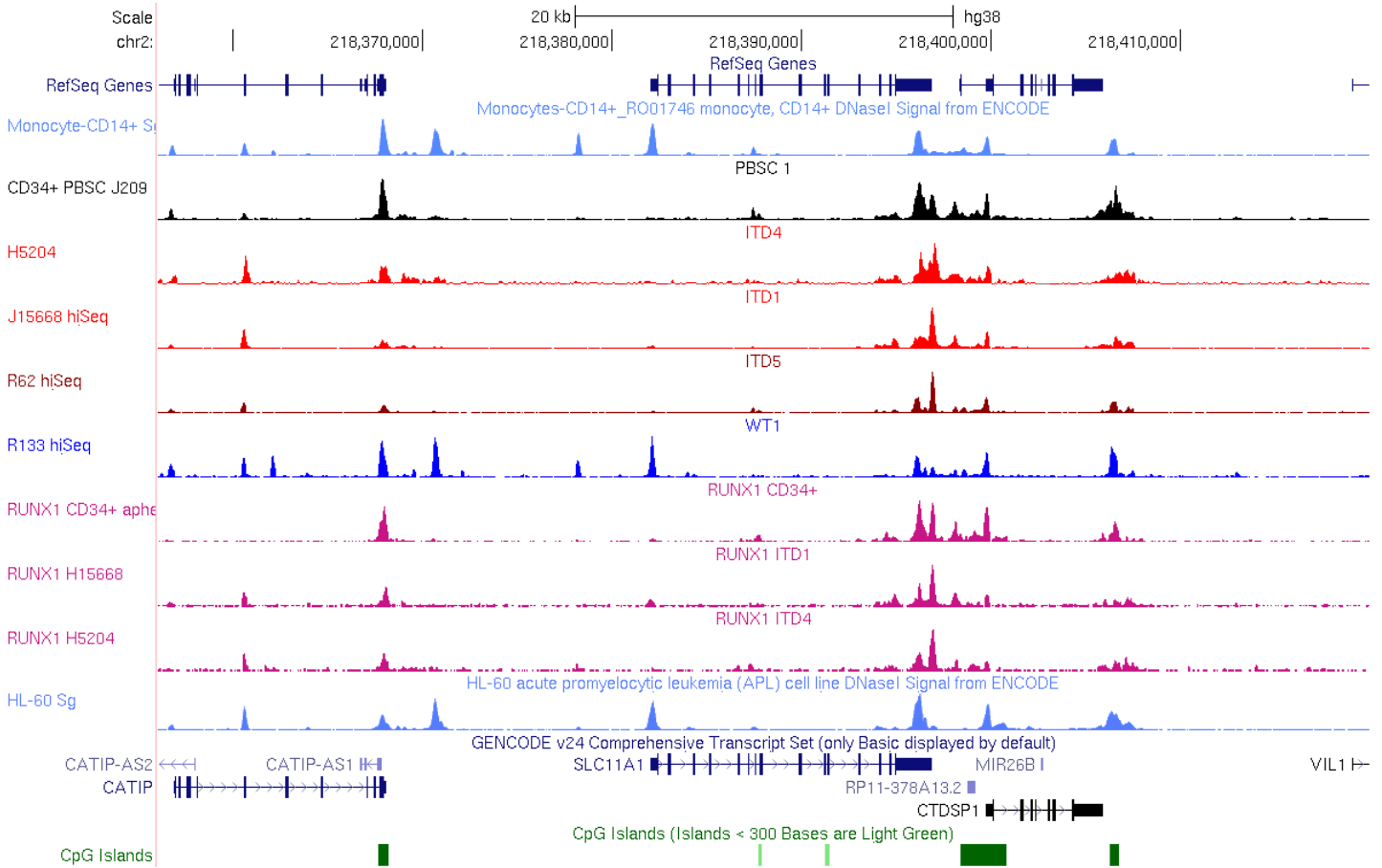


Figure S20. Effect of all *trans* retinoic acid ATRA on *NRAMP1* locus activity in AML (TSU1681MT) and APL (NB4). **A.** Gene expression and TF-specific ChIP-seq data for TSU-1621-MT AML [141]. *From top to bottom:* Chromosome 2 scale; DHS for HL-60 (M2 AML) and NB4 (M3 AML/APL); CpG islands; RNA-seq data in cells expressing ERG or not; ChIP-seq data for FLi1, RUNX1/AML1, SPI1/PU.1; FUS, ERG and RNA Pol II in cells treated with ATRA or not; UCSC gene descriptions. **B.** *NRAMP1* activity in NB4 cells ATRA-treated or not [146]. *From top to bottom:* ChIP-seq for RNA Pol II; RNA-seq data; ChIP-seq for K9me3; nuclease accessibility (*Nla* III; *Hpa* II, sensitive to DNA methylation); DNA methylation; ChIP-seq for K9/14ac; ChIP-seq data in untreated NB4 cells: p300 (HAT), H2A.Zac and K4me3. DHS in NB4 and HL-60 cells; ENCODE TF-ChIP-seq data; RefSeq gene depictions.

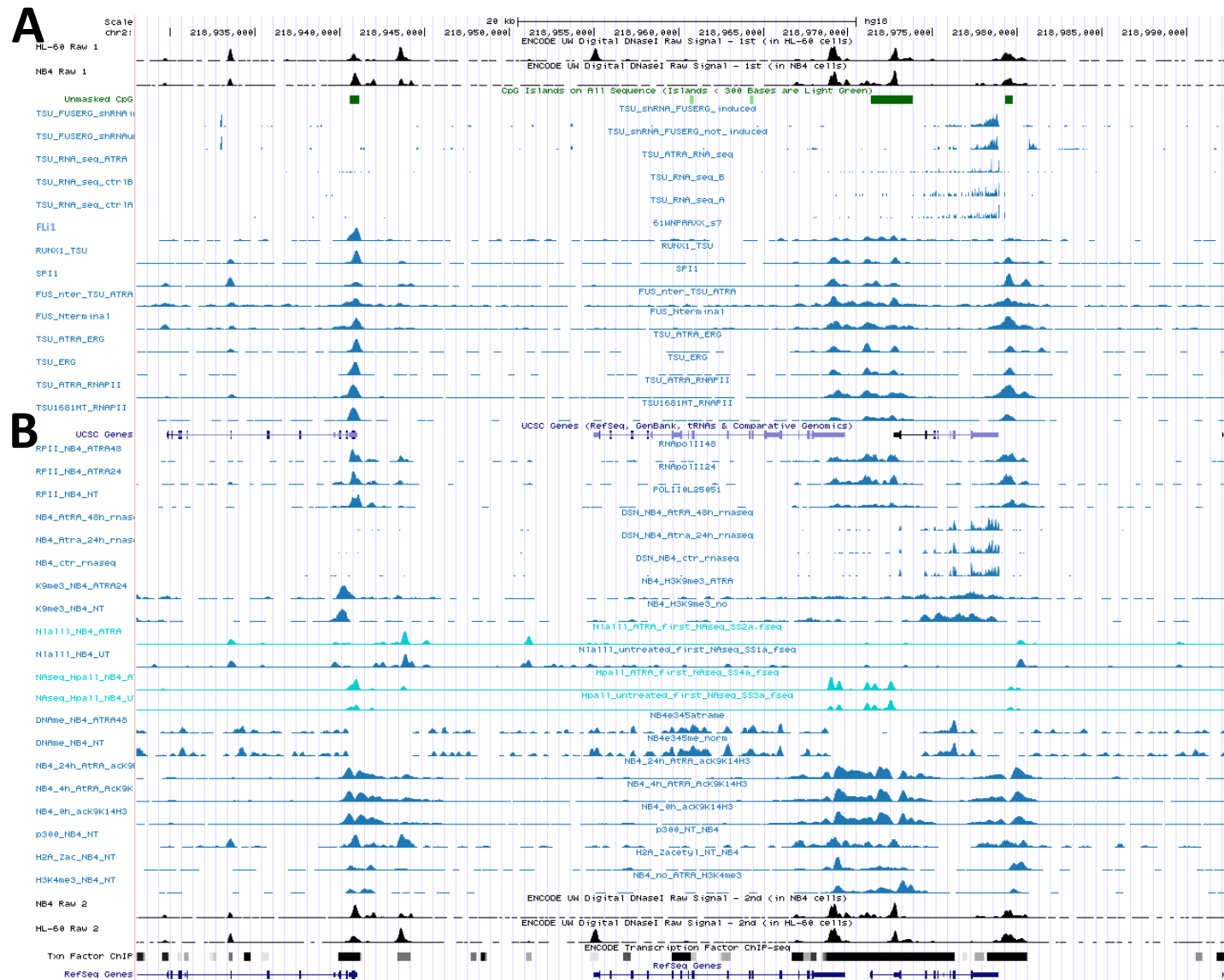


Figure S21. *NRAMP1* activity in Kasumi AML [142–44]. *From top to bottom:* chromosome 2 scale; CTCF-specific ChIP-seq (CD14⁺ MNs); RNA-seq for Kasumi cells expressing ERG or not; UCSC gene descriptions; acetylated histone-specific ChIP-seq data: K9/14ac in cells treated with MS275 (HDAC inhibitor; for 24, 4, or 0h); H4ac (untreated cells); ENCODE TF-specific ChIP-seq data; ChIP-seq for HDAC1 and HDAC2, N-CoR, HAT p300 (x2), GATA, LYL1, FLI1, TAL1, RUNX1/AML1 (AML blasts, Kasumi (x2) and NB4 cells); CpG islands; ChIP-seq for AML1-ETO fusion (x5); ENCODE DHS in CD14⁺ MNs (x2), HL-60 and NB4 AMLs, AML patients (2), mCD34, normal CD34⁺ HSPCs, CMK and K562 cells; RefSeq genes; CTCF-specific ChIP-seq (K562 cells); K4me1 and K27ac ChIP-seq data (CD14⁺ MNs and K562 cells); ChIP-seq for the TFs EGR2, PU.1 and C/EBPb in MN and MF [13]; K9ac, K4me2 and K4me3 ChIP-seq data (CD14⁺ MNs and K562 cells).

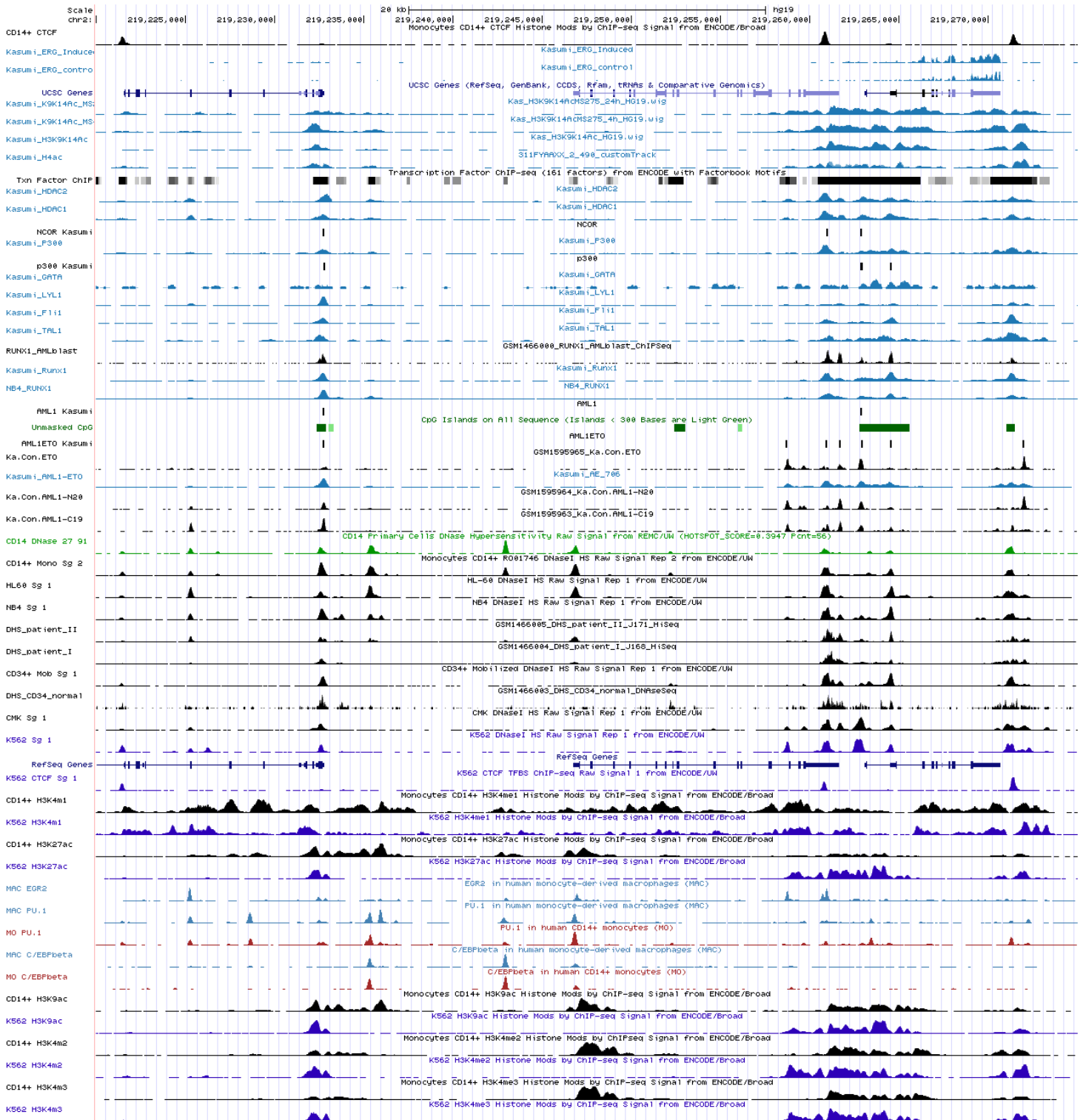


Figure S22. TF-specific ChIP-seq data for ME-1 AML [144]. *From top to bottom:* chromosome 2 scale; RefSeq genes; ENCODE TF-specific ChIP-seq data; DHS for HL-60 and NB4 APLs; ChIP-seq data specific for ERG, FLI1, TAL1, HEB, ELF1, PU.1, HDAC1, K9K14ac, HAT p300, TBP, RNA Pol II; DHS for NB4 and HL-60 APLs; CpG islands; RefSeq gene depictions.

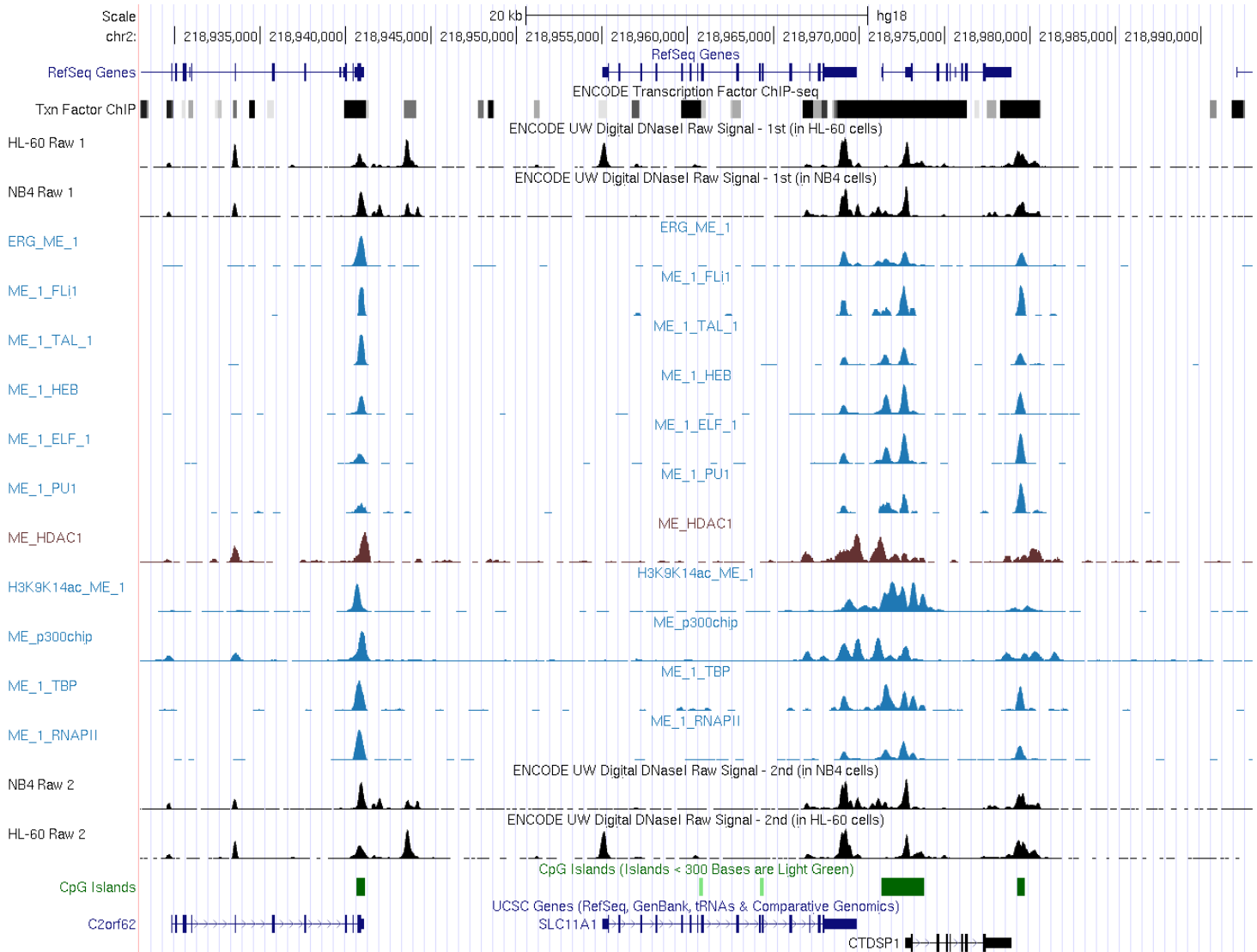
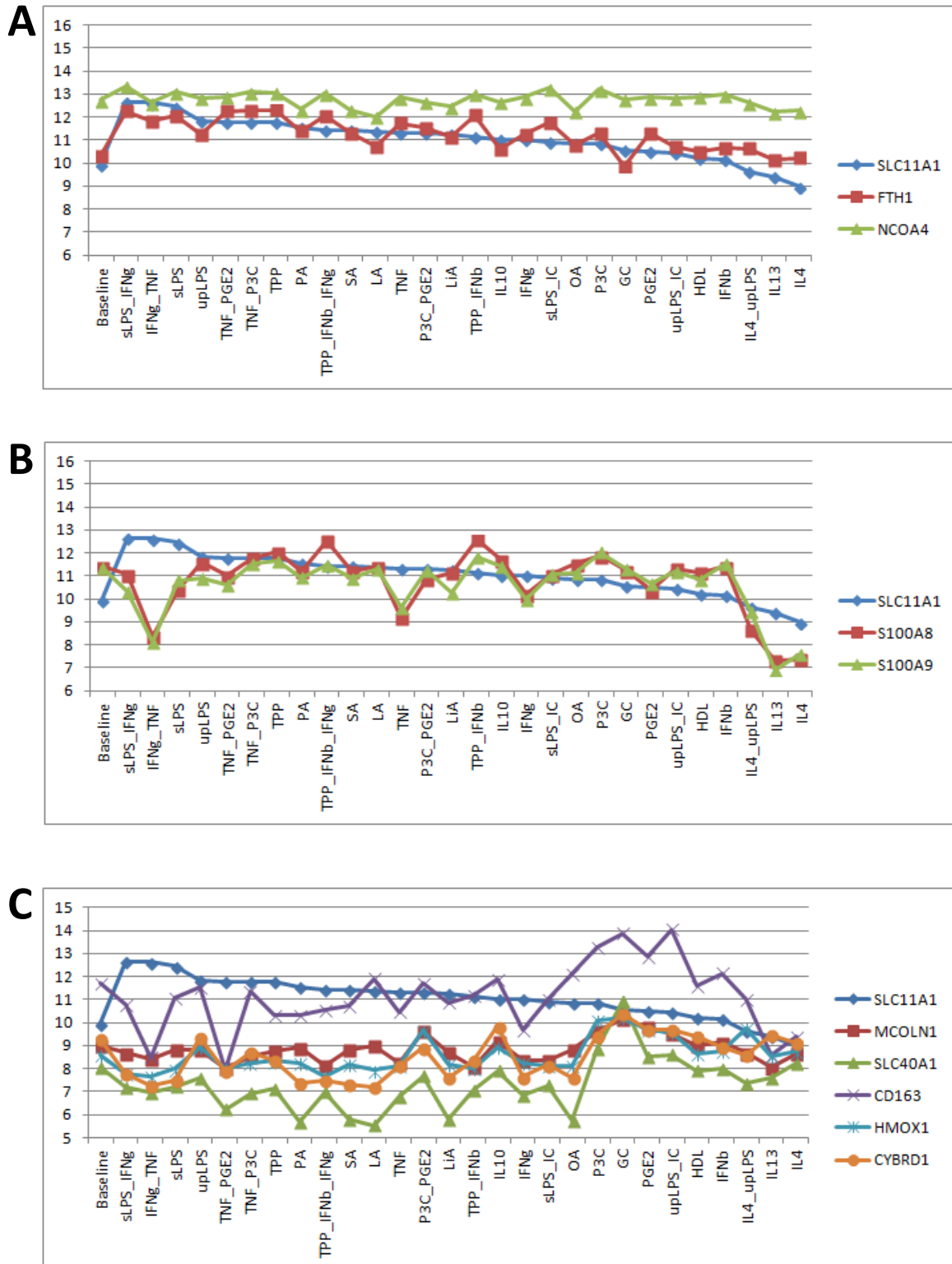


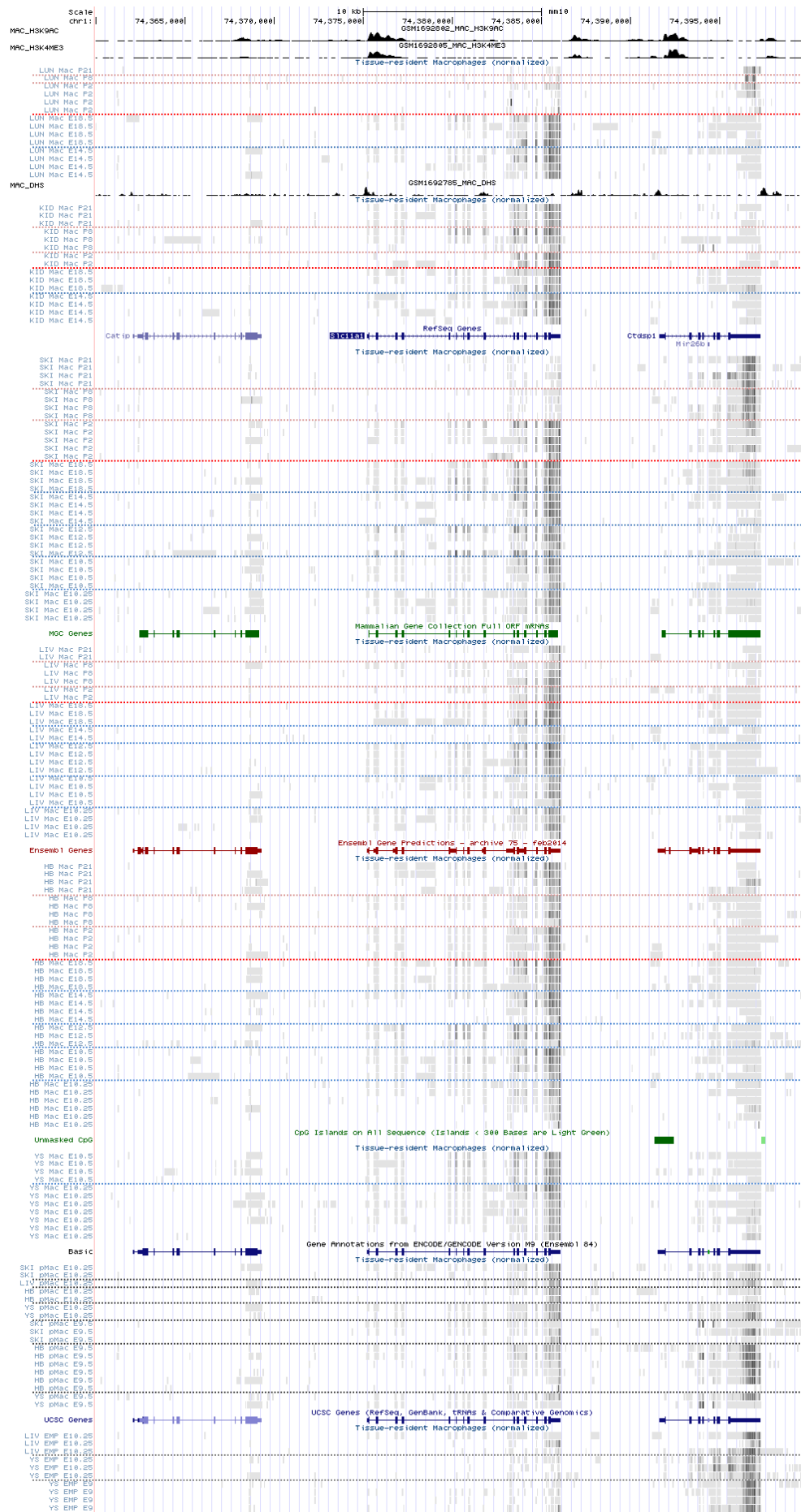
Figure S23. mRNA levels induced by 28 stimulation conditions producing MF phenotypes distributing across M1-M2 spectrum and ranked according to *NRAMP1* mRNA level (log2 transformed values, blue), decreasing from left to right, except for basal conditions (M-CSF or GM-CSF), at most left. **A.** Expression values are represented for *NRAMP1* and two other genes: *FTH1* (red) and *NCOA4* (green). **B.** Superimposition on *NRAMP1* profile of expression values for *S100A8* (red) and *S100A9* (green). **C.** Comparison of multiple profiles: *NRAMP1* (blue), *CD163* (purple), *MCOLN1* (red), *HMOX1* (cyan), *CYBRD1* (orange), *SLC40A1* (green) [132].



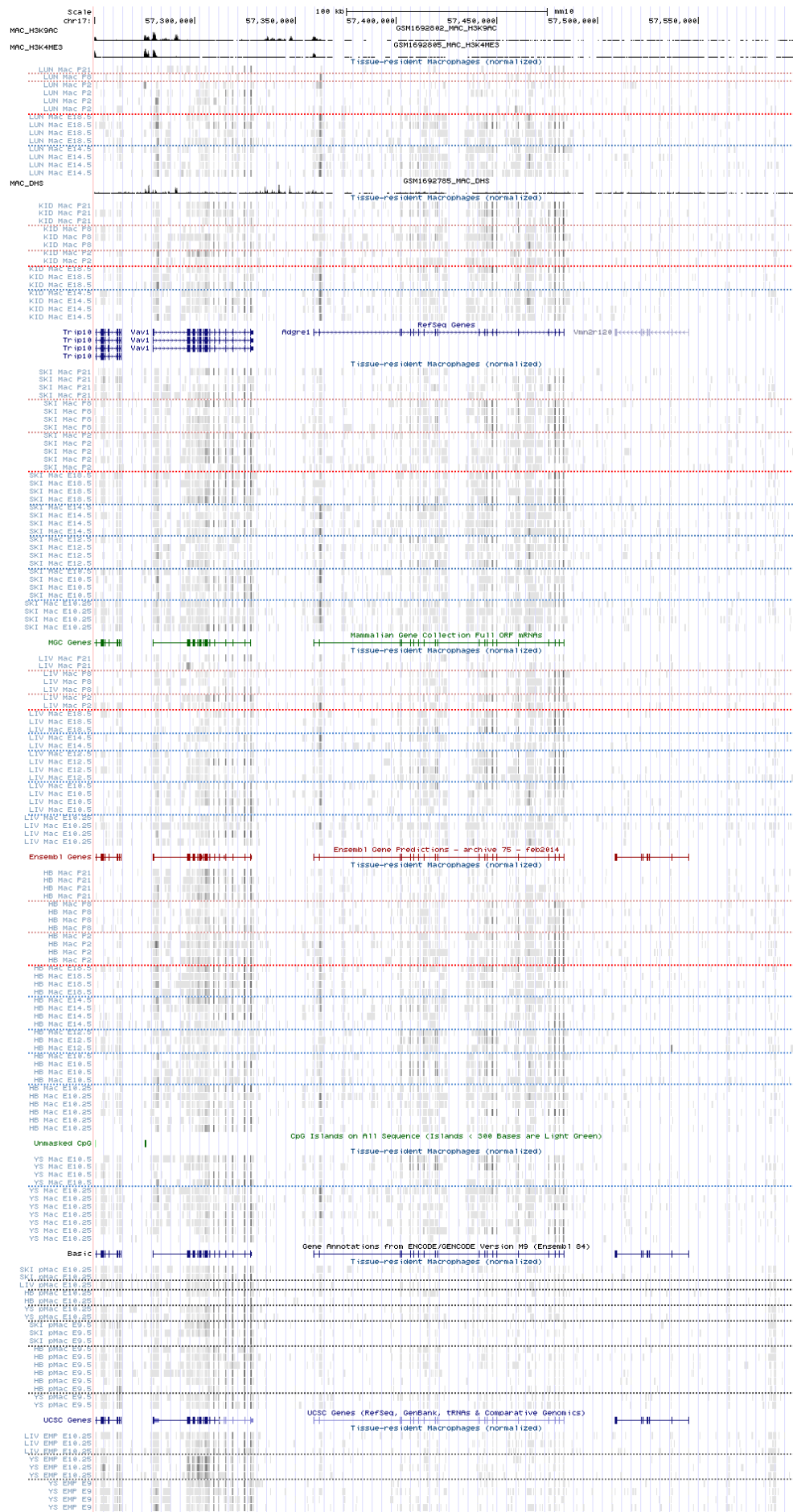
(next three pages)

Figure S24. RNA-seq analysis of gene expression during mouse embryogenesis and organogenesis: *Nramp1* (A), *Emr1* (F4/80; B) and *Cx3cr1* (C) [118]. Transcript levels for the genes *Catip*, *Nramp1/Slc11a1* and *Ctdsp1*, across several developmental steps, from embryo to adult, including i) tissue MFs (Mac E10.25 and E10.5 (YS, HB, LIV, SKI); Mac E12.5 (HB, LIV, SKI); Mac E14.5 and E18.5 (HB, LIV, SKI, KID, LUN); Mac P2, P8 and P21 (HB, LIV, SKI, KID, LUN)) and ii) their precursors (YS EMP E9 and E10.25; LIV EMP 10.25; pMac E9.5 (YS, HB, SKI); pMac E10.25 (YS, HB, LIV, SKI)). *Cx3cr1* expression is the most precocious (starting in EMP), followed by *Nramp1* (beginning in pMac) and *Emr1* (F4/80; first detected in tissue Mac). Also, *Nramp1* expression is specifically down regulated in MFs of adult skin and lung (P8, P21 and P2, P8 and P21, respectively).

A

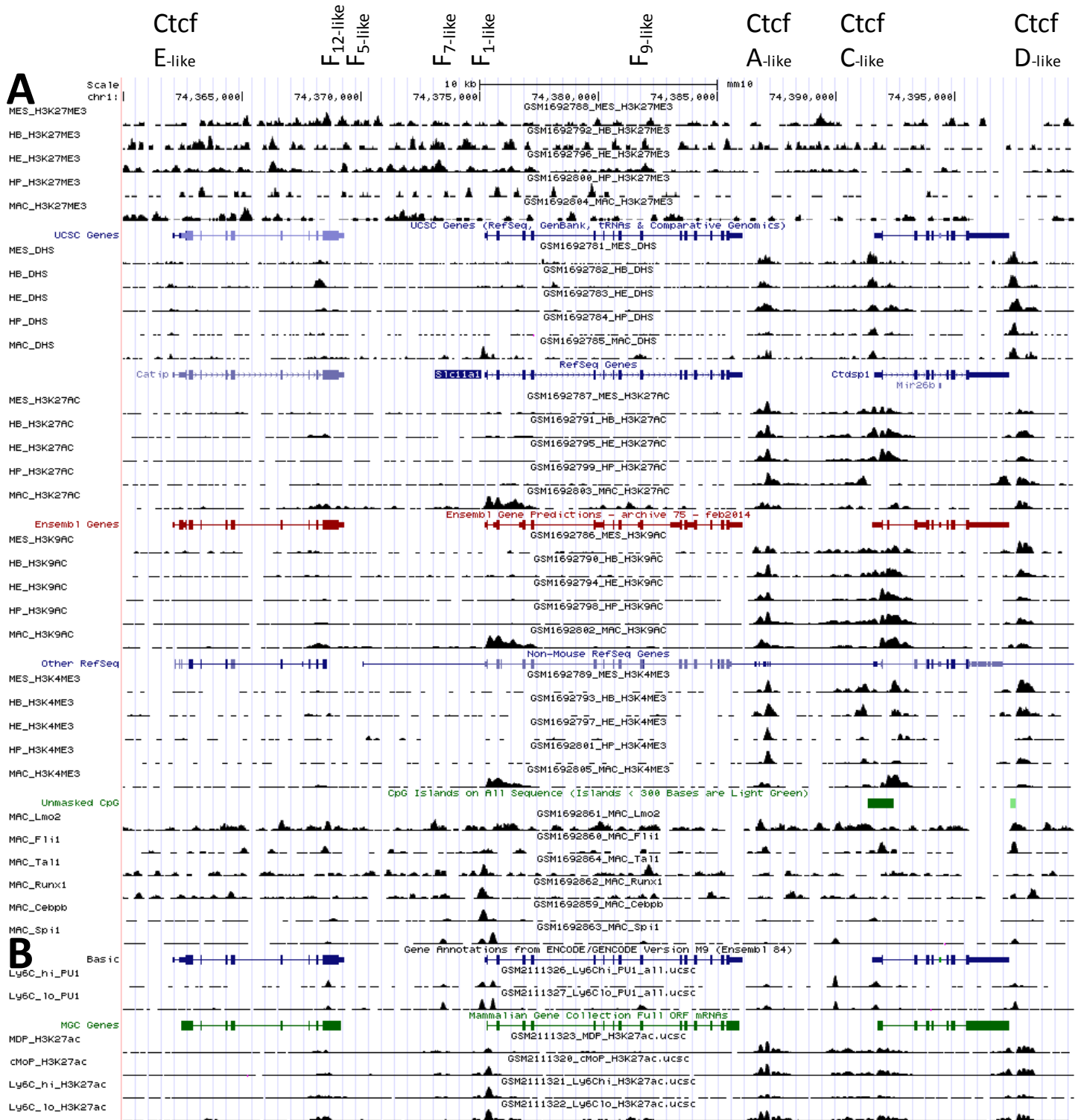


B



(next page)

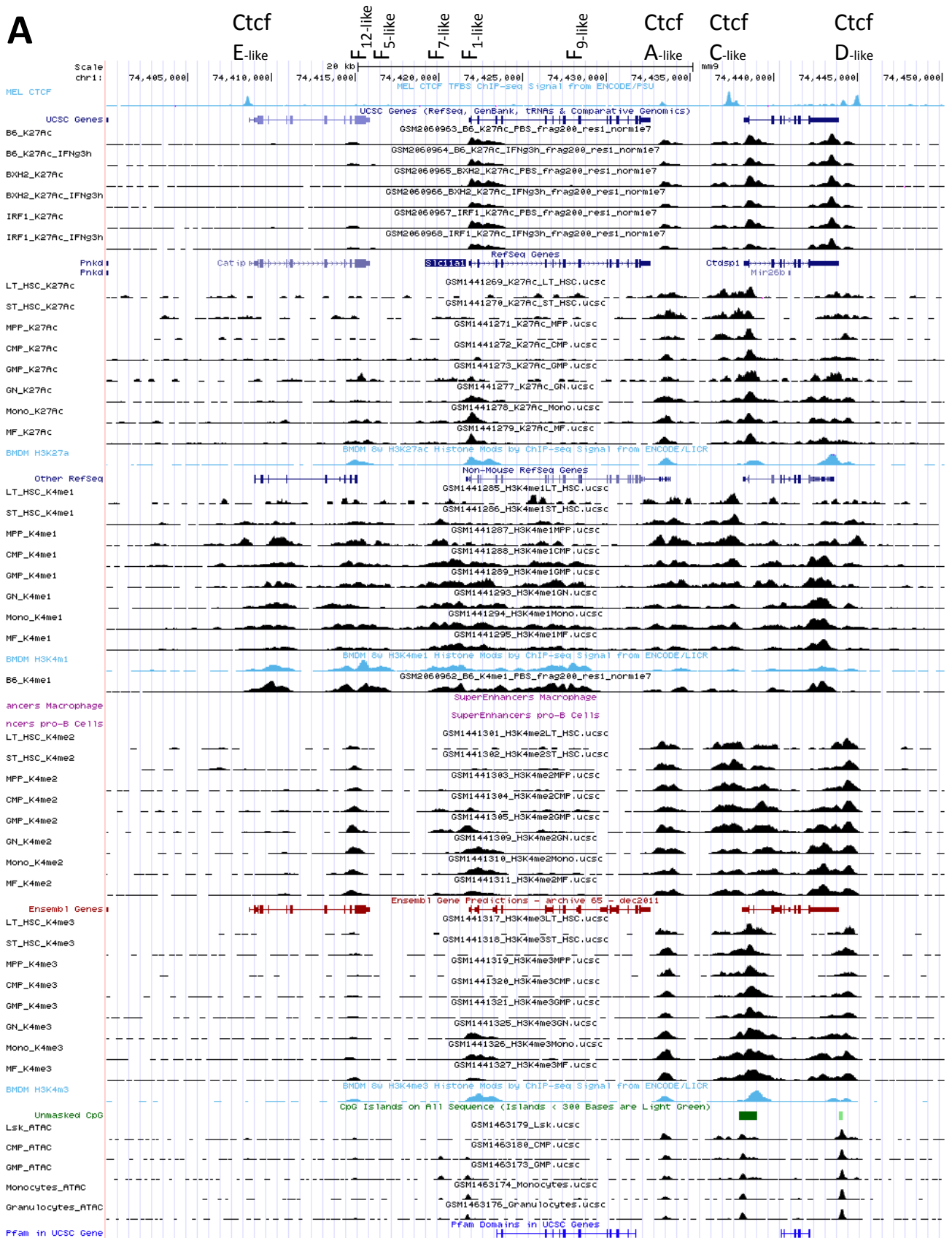
Figure S25. Epigenetic activity of *Nramp1* locus during primitive or definitive hematopoiesis. **A.** In vitro embryonic blood cell development: hematopoietic specification and differentiation starting from ESC [172]. Five successive stages of in vitro cell differentiation of ESC-derived embryoid bodies include: mesoderm cell (MES, day 1 of culture), hemangioblast (HB, day 2-3; smooth muscle, endothelial and hematopoietic potential), hemogenic endothelium (HE, day 4-5; endothelial and hematopoietic potential), CD41⁺ hematogenic precursor (HP, day 7) and Cd11b⁺ MFs (MAC). Reported epigenetic modifications comprise ChIP-seq analyses directed either at histone modifications or transcription factors, and DNase 1 hypersensitive sites (DHS), which together inform on chromatin activity. *From top to bottom:* candidate *Nramp1* regulatory elements, labeled by analogy with *NRAMP1* locus (cf Figure 7); mouse chromosome 1 scale; K27me3 (silent chromatin); UCSC genes; DHS (accessible chromatin); RefSeq genes; K27ac (activated chromatin); Ensembl genes; K9ac (transcriptionally active chromatin); Other RefSeq genes; K4me3 (transcriptionally active chromatin); CpG islands; association with TFs (Lmo2, Fli1, Tal1, Runx1, C/ebpb and Pu.1 (Spi1)). Note the presence of a cell-type-specific DHS spanning *Nramp1* TSS in MAC, which correlates with significant binding of few TFs in these cells only, including Pu.1, C/ebpb, Runx1, Tal1 but not Fli1 nor Lmo2 (Pu.1 binding was also detected in HP, with low intensity, data not shown). *Nramp1* TSS and downstream area is also prominently decorated with K27ac, K9ac and K4me3 marks, which indicate gene transcription in MAC. *Nramp1* TSS is labeled F1-like by analogy with human *NRAMP1* regulation; other predicted regulatory areas that appear similarly positioned to human cis-elements are labeled accordingly (F12-like, F5-like, F7-like and F9-like) as well as Ctf sites that either delimitate (E- and A-like) or flank *Nramp1* locus in downstream (C- and D-like). See text for details. DHS and histone marks also suggest limited activity at F12-, F7- and F9-like predicted determinants in MAC (and HB, F12-like). Epigenetic marks at *Ctdsp1* appear unrelated or inversely related to *Nramp1* activity. The above data indicate, as observed with *NRAMP1*, that *Nramp1* expression is restricted to late stages of myelo-monocytic differentiation and controlled by Pu.1 and C/ebpb TFs, consistent with the myeloid lineage determining roles of these factors. However, *Nramp1* TF binding profiles differ from what was observed with *NRAMP1* (e.g., Pu.1, C/ebpb, Runx1 and Tal1, compared to Figure 7 and Figures S19-22), implying regulatory divergence between mouse and human orthologous loci. **B.** *Nramp1* gene activity in vivo in bone marrow monocyte and progenitor subsets [150]. Cells were sorted using surface antigens (Cd155^{hi}, Cd117^{hi} Cd135⁺ and Ly6C^{hi} or Ly6C^{lo} for cMOP and MDP, respectively; Cd115^{hi}, Cd117^{lo}, Cd11c⁺ and Ly6C^{hi} or Ly6C^{lo} for Ly6C^{hi} and Ly6C^{lo} MNs, respectively). ChIP-seq for Pu.1 (Ly6C^{hi} and Ly6C^{lo} MNs) and K27ac (MDP, cMOP, Ly6C^{hi} and Ly6C^{lo} MNs).

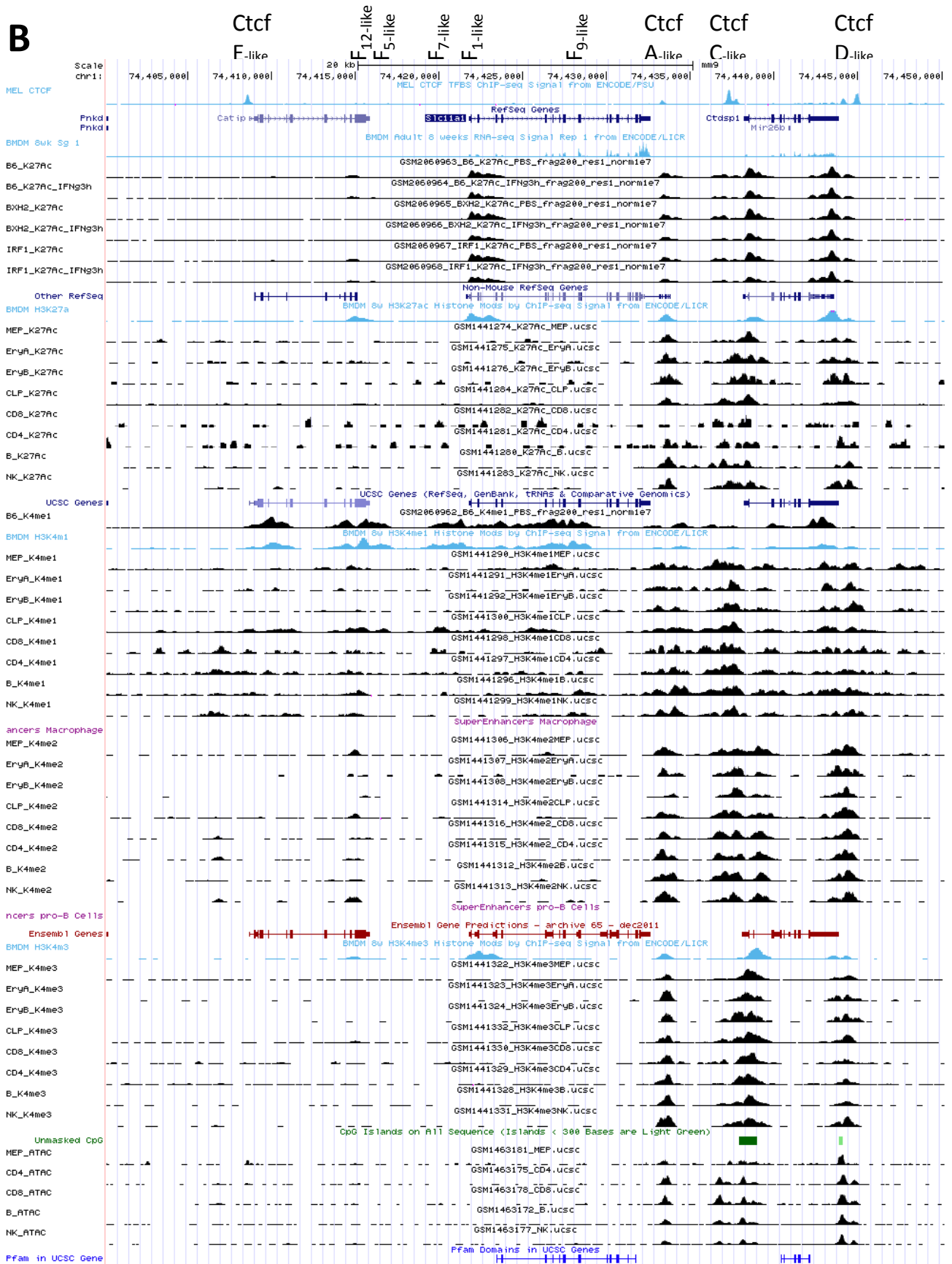


(next two pages)

Figure S26. De novo activation of *Nramp1* promoter in the myelo-monocytic lineage during definitive hematopoiesis in vivo (bone marrow) [25,173,177]. **A.** Myelopoiesis (long term HSC, LT-HSC; short-term HSC, ST-HSC; multipotent progenitor, MPP; CMP; GMP; GN; MN; MF). *From top to bottom:* candidate *Nramp1* regulatory elements labeled by analogy with *NRAMP1* locus (cf Figure 7); mouse chromosome 1 scale; Ctf sites (murine erythroleukemia cells); UCSC genes; ChIP-seq for K27ac in B6, BXH2 (Irf8 R294C) and *Irf1*^{-/-} BMDM, either naive or treated with Ifn-g; RefSeq genes; K27ac mark along myelopoiesis and in naive BMDM; other RefSeq genes; K4me1 mark along myelopoiesis and in naive BMDM (x2); super-enhancer tracks (MFs and pro-B cells); K4me2 mark along myelopoiesis; Ensembl genes; K4me3 mark along myelopoiesis and in naive BMDM; CpG islands; transposase accessible chromatin subjected to sequencing (ATAC-seq; Lsk (Lin⁻, Csa1^{hi}, Kit^{hi}, representing HSC), CMP, GMP, MN, GN); Pfam domains in UCSC genes. **B.** Erythropoiesis (MEPs; erythrocytic progenitors A, EryA (Ter119⁺, CD71⁺, high FSC); EryB (Ter119⁺, CD71⁺, low FSC) and lymphopoiesis (common lymphocytic progenitors, CLP; T lymphocytes Cd8⁺, CD8 and Cd4⁺, CD4; B lymphocytes, B; NK cells, NK). *From top to bottom:* candidate *Nramp1* regulatory elements labeled by analogy with *NRAMP1* locus (cf Figure 7); mouse chromosome 1 scale; Ctf sites (murine erythroleukemia cells); RefSeq genes; naive BMDM RNA-seq data; ChIP-seq for K27ac in B6, BXH2 (Irf8 R294C) and *Irf1*^{-/-} BMDM, either naive or treated with Ifn-g; Other RefSeq genes; K27ac mark in naive BMDM and along erythropoiesis and lymphopoiesis; UCSC genes; K4me1 mark in naive BMDM (2) and along erythropoiesis and lymphopoiesis; super-enhancer (macrophage track); K4me2 mark along erythropoiesis and lymphopoiesis; super-enhancer (pro-B cell track); Ensembl genes; K4me3 mark in naive BMDM and along erythropoiesis and lymphopoiesis; CpG islands; ATAC-seq (MEP, CD4, CD8, B, NK); Pfam domains in UCSC genes. Note *Nramp1* displays the stereotypical behavior of a de novo myelo-monocytic gene (similar to *S100A8* and *S100A9*, for instance) with stepwise acquisition of histone marks during differentiation: *Nramp1* promoter becomes marked at the root of the myeloid commitment point (during the MPP to CMP transition; K4me1 and K4me2 marks), then primed in GMP (K27ac) and activated in mature phagocytes (K4me3; GN, Mono and MF). ATAC-seq areas were detected at F7- and F1-like elements, both starting in CMP and either maintained in mature phagocytes (F1-like) or reduced after GMP (F7-like), suggesting that co-activation of F7- and F1-like elements represent an intermediate state. Absence of epigenetic signal along erythropoiesis and lymphopoiesis demonstrates the myelo-monocytic specificity of *Nramp1* expression.

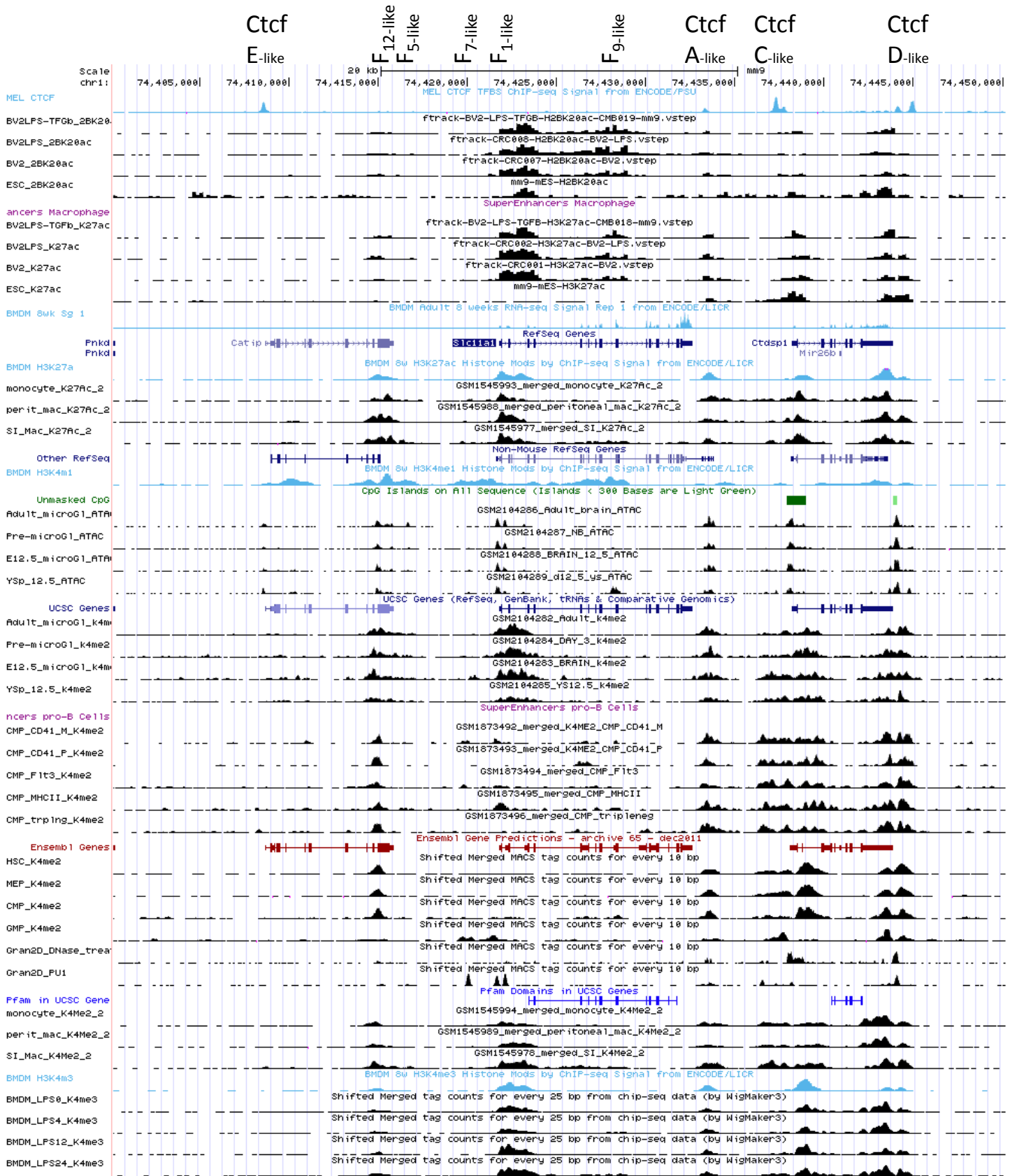
A





(next page)

Figure S27. In vitro and in vivo regulation of *Nramp1* gene expression [120,174–176,178,181]. *From top to bottom:* candidate *Nramp1* regulatory elements labeled by analogy with *NRAMP1* locus (cf Figure 7); mouse chromosome 1 scale; Ctf sites (murine erythroleukemia cells); H2BK20ac ChiP-seq analyses of microglial BV2 cells (naive or stimulated with LPS with or without Tgfb knockdown) and untreated ESC; super-enhancer track (macrophage); K27ac mark in microglial BV2 cells (naive or stimulated with LPS with or without Tgfb knockdown) and untreated ESC; naive BMDM RNA-seq data; RefSeq genes; K27ac mark in naive BMDM, tissue-resident MFs (peritoneum, small intestine) and blood MNs; Other RefSeq genes; naive BMDM K4me1 mark; CpG islands; ATAC-seq analyses of developmental stages of microglia (yolk sac EMP, early microglia (until E14), pre-microglia (few weeks post-partum); adult microglia); UCSC genes; K4me2 mark in developmental stages of microglia (yolk sac EMP, early microglia, pre- and adult microglia); super-enhancer track (pro-B cells); K4me2 mark in bone marrow CMP subtypes (CD41⁺; CD41⁻; Flt3⁺ Csf1r⁺; Irf8⁻ GFP⁺ MHCII⁺; Flt3⁻ Csf1r⁻ Irf8⁻ GFP⁻ MHCII⁻); Ensembl genes; K4me2 mark along in vitro definitive myelopoiesis (fetal liver HSC; MEP, CMP, GMP); DHS and Pu.1-specific ChiP-seq in GNs; Pfam domains in UCSC genes; K4me2 mark in tissue-resident MFs (peritoneum, small intestine) and blood MNs; K4me3 mark from naive BMDM and BMDM stimulated with LPS (0, 4, 12 and 24h). Note MF populations studied in vitro display limited activation of F12-like area (e.g., K27ac in BMDM and BN2 cells vs tissue-resident MFs and blood MNs). In contrast, tissue-resident MFs, including microglia, display high level of K27ac mark at F12-like element similar to TSS/F1-like; in addition, bone marrow myeloid progenitors show predominant K4me2 mark at F12-like element (four out of five CMP subtypes; HSC, MEP and CMP populations).



(next page)

Figure S28. Regulation of *Nramp1* expression in vitro: association with TFs and response to infectious stimuli [126,180,182,184,185,187,188]. *From top to bottom:* candidate *Nramp1* regulatory elements labeled by analogy with *NRAMP1* locus (cf Figure 7); mouse chromosome 1 scale; ATAC-seq analyses of BMDM either naive or stimulated with lipid A; RefSeq genes; ChIP-seq analyses of Irf3 and RelA in BMDM stimulated with lipid A; C/ebp sites (murine erythroleukemia cells); RNA-seq of naive BMDC; co-ChIP-seq analyses in BMDC (C/ebp or Pu.1 with H3, K27ac, K4me2 and K4me3); UCSC genes; ChIP-seq analyses of Irf8 and Pu.1 in Irf8⁺ Tot2 cells vs input; CpG islands; ChIP-seq analyses of Irf8 in BMDC (WT, *Batf3*^{-/-} and *Irf8*^{-/-}); Other RefSeq genes; RNA-seq of naive BMDM; ChIP-seq analyses of C/ebpa in macrophages, GMP and LSK (Lyn⁻, Sca1⁺, c-Kit⁻ HSC population [186]); Ensembl genes; H4K8ac and K27ac activation marks in RN2 cells (MLL-AF9) and K27ac mark in BMDM; ChIP-seq analyses in RN2 cells (MLL-AF9) of C/ebpa, C/ebpb, Pu.1, Erg, Myb, Fli1 and p300. Note i) increased accessibility of F9-like element in response to lipid A treatment, which corresponds to time-dependent chromatin association with both Irf3 and RelA; ii) association of F7-like element with C/ebpa and C/ebpb in cell types that do not express *Nramp1* (RN2 AML) or that express *Nramp1* at low level (BMDC, compare RNA-seq data between BMDC and BMDM, *Nramp1* transcript abundance relative to *Ctdsp1* mRNA levels) vs cells that express *Nramp1* at high level (e.g., C/ebpa in Mac; C/ebpb in ESCDM, Figure S25A); and iii) altered pattern of chromatin association of Irf8 in *Batf3*^{-/-} BMDC.

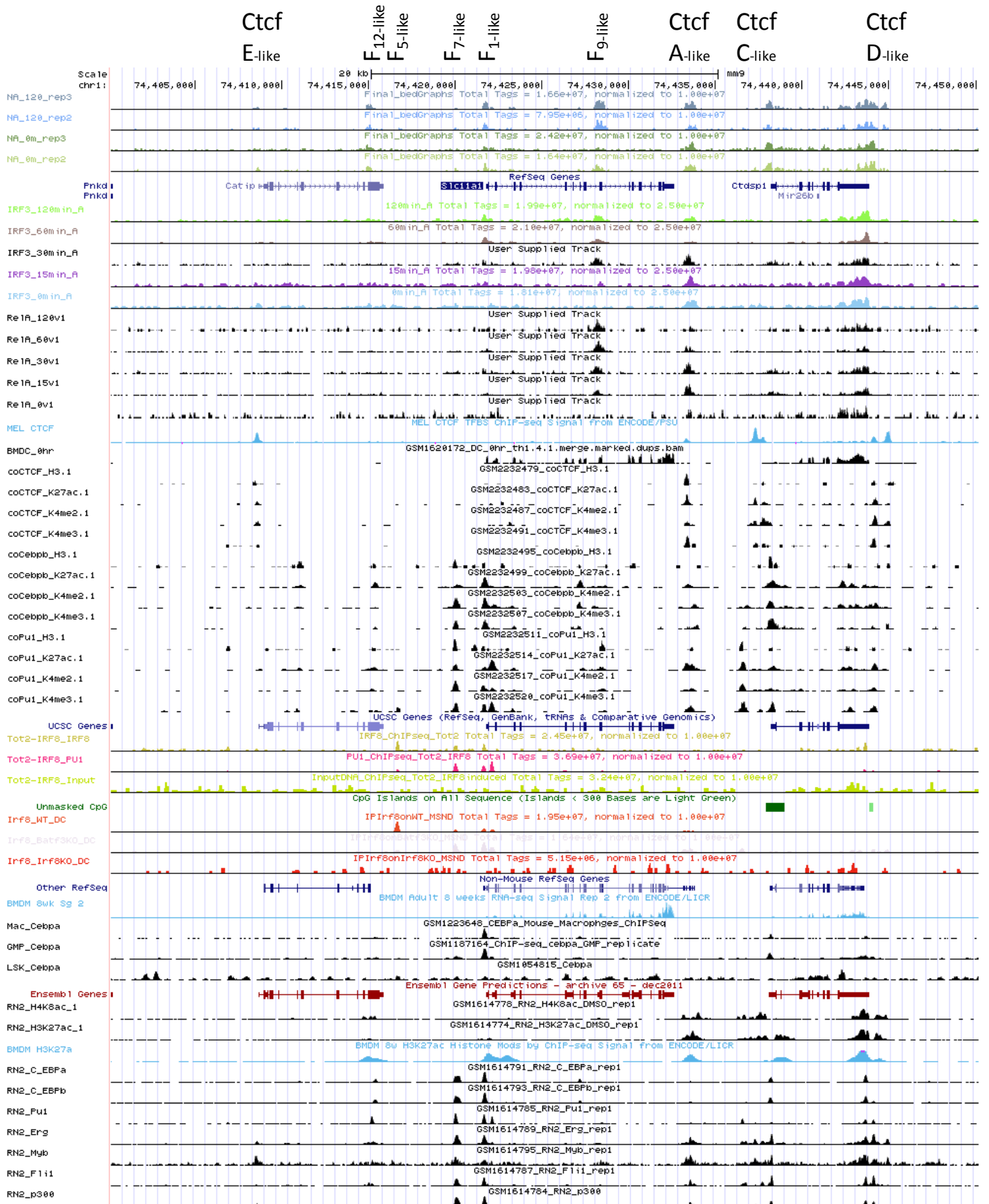


Table S1. Expression of macrophage iron genes

	Blood	Lung	Spleen	Mac [#] (max)	Ubq	TSS	Specificity [‡]	cS-E [§]
MN and PMN:								
<i>SLC11A1</i>	++	+	+	M1		no CpG no RPII NB4	MM	MN
<i>SLC40A1</i>	(+)	+	+	M2		CpG RPII NB4	(MM)	
<i>FTH1</i>	++	++	++	M1	+	CpG RPII NB4	(MM)	MN, Spl, Lng
<i>NCOA4</i>	++	++	++	++	+	CpG RPII NB4	(MM)	MN
<i>FTL</i>	++	++	++	++	+	CpG RPII NB4	(MM)	Spl
<i>S100A8</i>	++	++	++	M1		no CpG no RPII NB4	MM	
<i>S100A9</i>	++	++	++	+		no CpG no RPII NB4	MM	MN, Spl
<i>MCOLN1</i>	+	+	+	(M2)	low	CpG RPII NB4	(MM)	Spl
<i>SLC11A2</i>	+/-	(+)	(+)	+	low	CpG RPII NB4	(MM)	
<i>TFRC</i>	+/-	+	(+)	++	low	CpG RPII NB4	(MM)	
<i>SLC49A1</i>	+/-	+/-	+/-	(+/-)	vlo	CpG RPII NB4		
<i>PCBP1</i>	++	+	++	+	+	CpG RPII NB4	MM	MN, Spl, Lng
<i>PCBP2</i>	+	+	+	+	+	CpG RPII NB4		
<i>CYBRD1</i>	+/-	+	(+)	(M2)	+	CpG RPII NB4	(MM)	
<i>GAPDH</i>	++	++	++	(M1)	+	CpG RPII NB4	(MM)	MN, Spl, Lng
<i>SLC48A1</i>	+/-	+/-	+/-		vlo	CpG RPII NB4	(MM)	
MN and NOT in PMN:								
<i>CD91</i>	+/-	+	+	(+/-)	+	CpG w/o RPII NB4	(MM)	
<i>HMOX1</i>	+	+	++	(M2)		CpG w/o RPII NB4	MM	
<i>CD163</i>	+	+	+	M2	~lo	no CpG no RPII NB4	MM	
<i>SLC49A2</i>	+/-	(+)	(+)	(M2)	vlo	CpG RPII NB4 (wk)	MM	
<i>HAMP</i>	+/-	+/-	+/-	(M2)		no CpG no RPII NB4	MM	
<i>STEAP3</i>	+/-	(+)	+/-	+	vlo	CpG RPII NB4	(MM)	
<i>ITLN1</i>	+/-	+/-	+/-	(M2)		no CpG no RPII NB4	MM	
<i>SLC46A1</i>	0	+/-	(+)	+/-	vlo	CpG w/o RPII NB4		
PMN and NOT in MN:								
<i>LTF</i>	+	+/-	(+)	+/-		CpG (wk) w/o RPII NB4	MM	
<i>LCN2</i>	+	(+)	(+)	+/-		no CpG no RPII NB4		
NOT in PMN and MN:								
<i>SLC39A14</i>	0	(+)	+/-	+		CpG RPII NB4		
<i>TF</i>	0	0	0	+/-		CpG w/o RPII NB4		
<i>TFR2</i>	+/-	0	0	+/-		CpG RPII NB4	(MM)	
<i>LRP2</i>	0	+/-	0			CpG w/o RPII NB4		
<i>SCARA5</i>	0	+/-	0	+/-		no CpG no RPII NB4		
<i>CP</i>	0	+/-	(+)			no CpG w/ RPII NB4		
<i>HEPH</i>	+/-	(+)	(+)	+/-	vlo	no CpG no RPII NB4		
<i>PCBP3</i>	+/-	+/-	+/-	+/-	vlo	no CpG no RPII NB4	(MM)	
<i>PCBP4</i>	+/-	(+)	(+)	(+/-)	low	CpG w/o RPII NB4	MM	

[#]: compared to *SLC11A1* level; grey, no absolute values available

[§]: candidate super-enhancer domain, MN: monocytes; Spl: spleen; Lng: lung
GTEx expression levels (rpkm) [50]:

++ >200 >+ >20 >(+) >5 > +/- ;

Ubq + >20 >Ubq low >5 >Ubq vlo

[‡] MM: myelo-monocytic

Table S2. Macrophage iron gene mRNA expression levels [72].

Gene symbol	H1hESC	CD34	CD14	CD56	CD3	CD19
<i>SLC11A1</i>	1.47	47.82	7289.39	185.89	28.10	154.52
<i>SLC40A1</i>	1.70	7689.32	1681.30	1489.35	1621.83	709.28
<i>FTH1</i>	12478.75	52104.55	94947.65	27761.04	28520.66	14237.49
<i>NCOA4</i>	1944.77	15079.85	26725.16	8013.53	6585.10	6150.27
<i>FTL</i>	30226.82	36754.15	188509.89	32390.51	36014.26	36754.15
<i>S100A8</i>	0	3506.07	261343.64	2098.11	1047.96	3850.38
<i>S100A9</i>	0.60	4317.45	704402.40	3488.48	1958.10	4690.53
<i>MCOLN1</i>	1059.94	239.96	387.08	51.90	72.54	50.70
<i>SLC11A2</i>	1445.00	574.77	480.13	365.51	433.87	250.28
<i>TFRC</i>	2706.30	5399.45	752.67	967.00	1022.10	1378.73
<i>SLC49A1</i>	2125.13	230.89	328.92	286.20	298.91	321.54
<i>PCBP1</i>						
<i>PCBP2</i>	5600.73	17121.23	1967.30	3578.20	9041.77	2306.60
<i>CYBRD1</i>	466.81	1531.89	2657.30	711.21	73.03	138.75
<i>GAPDH</i>	630762.48	110615.15	61495.75	20351.54	25714.78	19192.00
<i>SLC48A1</i>	331.28	739.00	416.27	136.41	260.99	253.37
<i>CD91</i>	1814.69	49.40	2222.43	131.08	100.52	80.72
<i>HMOX1</i>	1690.77	43.28	8200.97	180.38	39.58	417.62
<i>CD163</i>	0.42	48.14	2233.87	91.48	12.53	35.68
<i>SLC49A 2</i>	471.22	30.48	884.00	38.14	52.87	31.47
<i>HAMP</i>	5.74	0	21.08	17.14	0	7.33
<i>STEAP3</i>	1866.10	228.60	193.95	46.93	1.76	45.01
<i>ITLN1</i>	0.41	6.06	139.99	5.36	0	1.74
<i>SLC46A1</i>	245.89	189.16	310.01	160.21	275.61	132.14
<i>LTF</i>	5.82	7.27	4.35	13.93	0	2.95
<i>LCN2</i>	11.24	22.64	5.11	88.17	0	40.74
<i>SLC39A14</i>	4531.96	212.85	46.63	130.75	224.29	148.33
<i>TF</i>	0.33	10.64	8.46	14.86	10.02	3.50
<i>TFR2</i>	75.49	1065.89	17.02	41.36	72.79	26.66
<i>LRP2</i>	82.61	3.59	1.23	0	1.01	0
<i>SCARA5</i>	0.63	0	8.06	17.55	0	30.25
<i>CP</i>	6.48	508.59	29.65	50.96	31.17	36.96
<i>HEPHL1</i>	9.82	6.35	17.26	59.32	6.05	40.86
<i>PCBP3</i>	34.13	92.03	0	18.24	20.22	15.29
<i>PCBP4</i>	893.95	132.47	29.58	195.63	299.66	264.89

